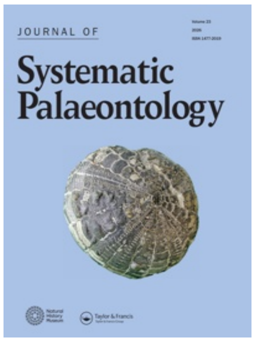

Journal of Systematic Palaeontology

ISSN: 1477-2019 (Print) 1478-0941 (Online) Journal homepage: www.tandfonline.com/journals/tjsp20

A new saurolophine hadrosaurid (Dinosauria: Ornithopoda) from the Upper Cretaceous of South China, providing further support for the possible Asian origin of Brachylophosaurini

Han Yao, Wenjiang Qiu, Juan Yu, Ling Yang, Huimin Wang, Shenghua Cao, Kui Zhao, Mengyuan Xu, Guo Shi, Fasheng Lou, Cuimin Zeng, Pikun Lu, Rui Wu, Xing Xu, Fenglu Han & Hai Xing

To cite this article: Han Yao, Wenjiang Qiu, Juan Yu, Ling Yang, Huimin Wang, Shenghua Cao, Kui Zhao, Mengyuan Xu, Guo Shi, Fasheng Lou, Cuimin Zeng, Pikun Lu, Rui Wu, Xing Xu, Fenglu Han & Hai Xing (2026) A new saurolophine hadrosaurid (Dinosauria: Ornithopoda) from the Upper Cretaceous of South China, providing further support for the possible Asian origin of Brachylophosaurini, Journal of Systematic Palaeontology, 24:1, 2635569, DOI: 10.1080/14772019.2026.2635569

To link to this article: https://doi.org/10.1080/14772019.2026.2635569

Journal of Systematic Palaeontology, 2026
Vol. 24, No. 1, 2635569
http://dx.doi.org/10.1080/14772019.2026.2635569

A new saurolophine hadrosaurid (Dinosauria: Ornithopoda) from the Upper Cretaceous of South China, providing further support for the possible Asian origin of Brachylophosaurini

Han Yao[a‡], Wenjiang Qiu[b‡], Juan Yu[c], Ling Yang[c], Huimin Wang[b], Shenghua Cao[b], Kui Zhao[b], Mengyuan Xu[d], Guo Shi[d], Fasheng Lou[e], Cuimin Zeng[c], Pikun Lu[f], Rui Wu[a,g], Xing Xu[h,i], Fenglu Han[a]* and Hai Xing[j,k]*

[a]*School of Earth and Planetary Sciences, China University of Geosciences, Wuhan 430074, China;* [b]*Basic Geological Survey Institute of Jiangxi Geological Survey and Exploration Institute, Nanchang, 330030, China;* [c]*Jiangxi Geological Museum, Nanchang, 330002, China;* [d]*School of Earth Sciences, East China University of Technology, Nanchang 330013, China;* [e]*Institute of Jiangxi Geological Survey and Exploration Institute, Nanchang 330030, Nanchang 330013, China;* [f]*Shenhao Geological Exploration Company, Ganzhou 341000, China;* [g]*Shanghai Natural History Museum, Shanghai Science and Technology Museum, Shanghai, 200041, China;* [h]*Centre for Vertebrate Evolutionary Biology, Yunnan University, Kunming, 650091, China;* [i]*Key Laboratory of Vertebrate Evolution and Human Origins, Institute of Vertebrate Paleontology and Paleoanthropology, Chinese Academy of Sciences, Beijing, 100044, China;* [j]*National Natural History Museum of China, Beijing 100050, China;* [k]*Beaty Centre for Species Discovery and Palaeobiology Section, Canadian Museum of Nature, Ottawa K1P 6P4, Canada*

(Received 28 September 2025; accepted 21 January 2026)

A new saurolophine hadrosaurid, *Gongshuilong fanwei*, is named and described here based on a series of largely disarticulated bone elements from the middle of the Upper Cretaceous Lianhe Formation in Ganzhou City, Jiangxi Province, South China. This taxon is diagnosed by a unique combination of traits, including an elevated anterodorsal process of the maxilla which is slightly longer than the anteroventral one, dentary tooth crowns ornamented with a median primary ridge and relatively small marginal denticles, an extremely truncated edentulous region of the dentary, an anteroposteriorly wide ventral process of the postorbital, a poorly developed deltoid ridge on the lateral surface of the scapula, and markedly elongate, posterodorsally directed neural spines of the posterior caudal vertebrae that are moderately recurved. Phylogenetic analysis yielded a polytomy at the base of Brachylophosaurini within Saurolophinae, which is formed by *Wulagasaurus*, *Gongshuilong*, *Acristavus* and the clade of *Maiasaura* + (*Probrachylophosaurus* + *Brachylophosaurus*). *Gongshuilong* is the first reported hadrosaurid genus from South China and is the second taxon of Brachylophosaurini found in Asia. Its discovery increases the possibility of the Asian origin for Saurolophinae and Brachylophosaurini, based on biogeographical analysis for ancestral areas using the Bayesian binary method.

https://zoobank.org/urn:lsid:zoobank.org:pub:221FCD08-59F6-4637-9BC5-D50EB904EE2C

Keywords: Brachylophosaurini; Ganzhou Basin; Hadrosauridae; Late Cretaceous; Saurolophinae

Introduction

Hadrosauroidea, defined as to the most inclusive clade containing *Hadrosaurus foulkii* but not *Iguanodon bernissartensis*, is a globally distributed herbivorous lineage of large-sized ornithischian dinosaurs, which was thriving and diverse during the entire Cretaceous (Dai et al., 2025; Horner et al., 2004; Prieto-Márquez, 2010a; You et al., 2003). The fossil record of Hadrosauroidea is geographically extensive, encompassing articulated and disarticulated bones, eggs and other remains (Currie et al., 1991; Lull & Wright, 1942; Prieto-Márquez, 2010b; Wing & Sues, 1992). This clade is remarkable for the distinctly expanded duck-like bills and more complex dental batteries (Horner et al., 2004; Prieto-Márquez, 2010b). Hadrosauridae material has been retrieved worldwide, including the Americas, Europe, Asia, Africa and even Antarctica (Horner et al., 2004; Longrich et al., 2021). Hadrosauridae is particularly well represented, with high diversity during the Campanian and Maastrichtian of North America and Asia (Godefroit et al., 2008; Lund & Gates, 2006). The success of hadrosaurids can be primarily attributed to their highly specialized and efficient plant-processing feeding system that includes the robust, transversely movable lower jaw and complicated dental batteries. These configurations are useful for the processing of tough vegetation via long-axis rotation of the mandibular rami (Cuthbertson et al., 2012; Nabavizadeh 2016; Ostrom 1961; Rybczynski et al., 2008). Hadrosauridae

---

*Corresponding authors: Emails: hanfl@cug.edu.cn; xinghaiivpp@gmail.com
‡These authors contributed equally to this paper.

consists of two major clades, namely Saurolophinae bearing solid crests or flat-headed skulls and Lambeosaurinae having hollow cranial crests (Horner et al., 2004; Prieto-Márquez, 2010b; H. Xing, Wang et al., 2014).

To date, six formally named hadrosaurid dinosaurs have been found in China, which have been limited to northern areas of the country (Table 1). Two stratigraphical ranges and corresponding locations stand out because of their abundant hadrosaurid fossil record: the Yuliangzi Formation (?early to middle Maastrichtian) in Jiayin and Xunke, Heilongjiang Province (Godefroit et al., 2008; H. Xing et al., 2021), and the Hongtuya (?middle to late Campanian) and Jingangkou (?late Campanian to early Maastrichtian) formations in Zhucheng and Laiyang, Shandong Province (H. Xing, Zhao et al., 2014; Zhang et al., 2019). The Yuliangzi Formation has yielded the saurolophine *Wulagasaurus dongi* and the lambeosaurines *Charonosaurus jiayinensis* and *Amurosaurus riabinini* (Godefroit et al., 2000, 2008; H. Xing et al., 2021). In Shandong Province, the lambeosaurine *Tsintaosaurus spinorhinus* and the saurolophine *Laiyangosaurus youngi* were recovered from the Jingangkou Formation and the saurolophine *Shantungosaurus giganteus* was reported from the Hongtuya Formation. In addition to China, hadrosaurids have been reported from several regions across Asia. These include *Aralosaurus tuberiferus* and *Jaxartosaurus aralensis* from Kazakhstan, *Olorotitan arharensis* and *Kerberosaurus manakini* from Far Eastern Russia, and *Saurolophus angustirostris* from Mongolia (Bolotsky & Godefroit, 2004; Godefroit, Alifanov et al., 2004; Godefroit et al., 2012; Maryańska & Osmólska, 1984; Rozhdestvensky, 1968). However, all of these occurrences lie in the more northerly regions of the continent. By contrast, the specific hadrosaurid fossil record in southern areas of China is particularly sparse, although some early-diverging hadrosauroid substitutes (such as *Nanningosaurus dashiensis* and *Qianjiangsaurus changshengi*) have been recovered.

Here we provide an osteological description and a phylogenetic assessment on a new saurolophine hadrosaurid from South China, with global comparisons to other hadrosauroids. The study is based on dozens of largely disarticulated skull and postcranial elements recovered from a single bonebed (catalogued as BGS-JX F001) within the middle of the Upper Cretaceous (Maastrichtian) Lianhe Formation at the Zhutongkeng locality, Shahe Town, Zhanggong District, Ganzhou City, Jiangxi Province (Fig. 1). The fossil elements were preliminarily exposed in March 2021 during construction activities in the industrial zone of Ganzhou, Jiangxi Province. Following official approval by the General Office of the Ministry of Natural Resources of Jiangxi Province, China, in April 2021 (Document No. 685 [2021]), a protective fossil excavation was carried out by the Basic Geological Survey Institute of the Jiangxi Geological Survey and Exploration Institute (BGS-JX), and Jiangxi Geological Museum (JXGM), with the retrieval of all studied material. In the Ganzhou area, two brief studies on hadrosauroid material were published previously, with one study identifying a possible hadrosaurid individual mainly based on a partial dorsal series with articulated ribs recovered from the Hekou Formation (L. Xing et al., 2021), and the other describing two embryo-bearing eggs, from the same formation (L. Xing et al., 2022); however, the specific taxonomic assignments and stratigraphical horizons regarding these specimens remain unknown. The discovery of the new saurolophine hadrosaurid greatly expands the depth of our understanding of the early radiation of Saurolophinae and late evolution of Hadrosauridae, both taking place in Asia, and helps elucidate the geographical origin and intercontinental dispersal of Brachylophosaurini.

Geological setting

The Ganzhou Basin, filled with Upper Cretaceous alluvial, fluvial to lacustrine deposits and volcanic deposits produced by intermittent volcanism, is located in southern Jiangxi Province and extends in a north-east–south-west direction. The Upper Cretaceous continental strata in the Ganzhou Basin had traditionally been divided into the lower Ganzhou Formation and the upper Nanxiong Formation. Most vertebrate fossils were collected from the upper Nanxiong Formation which was dated to the Maastrichtian (C. Li et al., 2019; Lü et al., 2016; Zheng et al., 2024). However, in recent studies, the strata were further subdivided into the lower Ganzhou Group composed of the Maodian and Zhoutian formations, and the upper Guifeng Group consisting of the Hekou, Tangbian and Lianhe formations in ascending order (Fig. 1C) (T. Li et al., 2017).

Due to historical and technical limitations, the relative ages of most formations from the Ganzhou Basin have been constrained by lithostratigraphical correlations and biostratigraphical evidence, whereas absolute geochronological data are available only from the Maodian Formation (T. Li et al., 2017; Ling, 1996; Zhong et al., 2002). The isotopic ages obtained from the Maodian Formation provide the principal chronological framework for inferring the age of the other formations, including the Lianhe Formation. The Maodian Formation mainly consists of coarse conglomerates and pebbly sandstones interbedded with basalt and tuffaceous andesite (T. Li et al., 2017; Ling, 1996; Zhong

Table 1. Distribution and stratigraphic context of six formally named hadrosaurid dinosaurs in China.

Classification	Taxon	Locality and horizon	References
Lambeosaurinae	*Amurosaurus riabinini*	Wulaga Town, Jiayin County, Heilongjiang Province. Upper Yuliangzi Formation (Udurchukan Formation in Russia), middle Maastrichtian.	Bolotsky & Godefroit, 2004; Godefroit et al., 2008; H. Xing et al., 2021
Lambeosaurinae	*Charonosaurus jiayinensis*	Jiayin County, Heilongjiang Province. Lower Yuliangzi Formation (Udurchukan Formation in Russia), early Maastrichtian.	Godefroit et al., 2000, 2011
Lambeosaurinae	*Tsintaosaurus spinorhinus*	Jingangkou, Laiyang City, Shandong Province. Jingangkou Formation, late Campanian to early Maastrichtian.	Z. Yang, 1958; Zhang et al., 2021
Saurolophinae	*Laiyangosaurus youngi*	Jingangkou, Laiyang City, Shandong Province. Jingangkou Formation, late Campanian to early Maastrichtian.	Zhang et al., 2019
Saurolophinae	*Shantungosaurus giganteus*	Kugou, Zhucheng City, Shandong Province. Hongtuya Formation, middle to late Campanian.	Hu, 1973; H. Xing, Zhao et al., 2014
Saurolophinae	*Wulagasaurus dongi*	Wulaga Town, Jiayin County, Heilongjiang Province. Upper Yuliangzi Formation (Udurchukan Formation in Russia), middle Maastrichtian.	Godefroit et al., 2008; H. Xing et al., 2012

et al., 2002). It yielded a K-Ar radiometric age of 85.9 Ma (Ling, 1996), while quartz electron spin resonance (ESR) dating indicated the age was between 96.5 and 87.5 Ma (Cenomanian–Coniacian) (Zhong et al., 2002). The overlying Zhoutian Formation developed a terrestrial facies lake basin which is composed of fine-grained siltstones and mudstones, interbedded with several gypsum layers. The relationship between the sequences of these formations displays conformable contact. In the Ganzhou Group, vertebrate fossils were mainly collected from the Zhoutian Formation, which is exposed in the north-east part of Ganxian district and Longling town, Ganzhou City, including the squamates *Conicodontosaurus kanhsienensis* (T. Li et al., 2017; C. Yang 1973), Sauropoda (Han et al., 2024; T. Li et al., 2017; Lü et al., 2013) and Oviraptoridae (T. Li et al., 2017; Wei et al., 2013). The lower Maodian Formation has yielded an assemblage consisting mainly of dinosaur eggs that were preserved in the coarse-grained conglomerates and pebbly sandstone (R Wu & F. Han, pers. obs.).

Vertebrate fossils were also documented from the overlying Guifeng Group, predominantly within the Hekou and Tangbian formations. Various vertebrate remains, including the squamates *Yechilacerta yingliangia* (L. Xing et al., 2023) and *Caninosaurus ganzhouensis* (M. Wang et al., 2025); the crocodilian *Eurycephalosuchus gannanensis* (X. C. Wu et al., 2023); the mammals *Yubaatar qianzhouensis* (J. Hu & Han, 2021) and *Erythrobaatar ganensis* (Jin et al., 2023); and the dinosaurian skeleton and eggs mentioned previously (L. Xing et al., 2020, 2021, 2022; R. Wu, Lou et al., 2024), have been extensively reported over the past two decades.

The hadrosaurid material reported here was collected from the Upper Cretaceous Lianhe Formation, Guifeng Group. The Lianhe Formation is composed of red conglomerates, pebbly sandstones interbedded with fine-grained siltstones and mudstones, and displays conformable contact with the lower Tangbian Formation (T. Li et al., 2017). The depositional setting of the former formation is interpreted as fluvial and alluvial deposition (Xiao et al., 2013). The Lianhe Formation yields gastropods and egg fossils and can be dated to the Maastrichtian according to the spore and pollen assemblages (T. Li et al., 2017). Its deposits are widely distributed in areas of the Shahe Industrial Zone and Ganzhou Railway Station (Supplemental material Fig. S1). A large-sized nanhsiungchelyid *Xianyuechelys yingliangi* (Ke et al., 2024) and the ootaxon *Gannanoolithus yingliangi* (R. Wu, Niu et al., 2024) have also been collected from the Lianhe Formation in recent years.

Institutional abbreviations

AENM, Amur Natural History Museum, Russian Academy of Sciences, Blagoveschensk, Russia; **BGS-JX**, Basic Geological Survey Institute of Jiangxi Geological Survey and Exploration Institute, Nanchang,

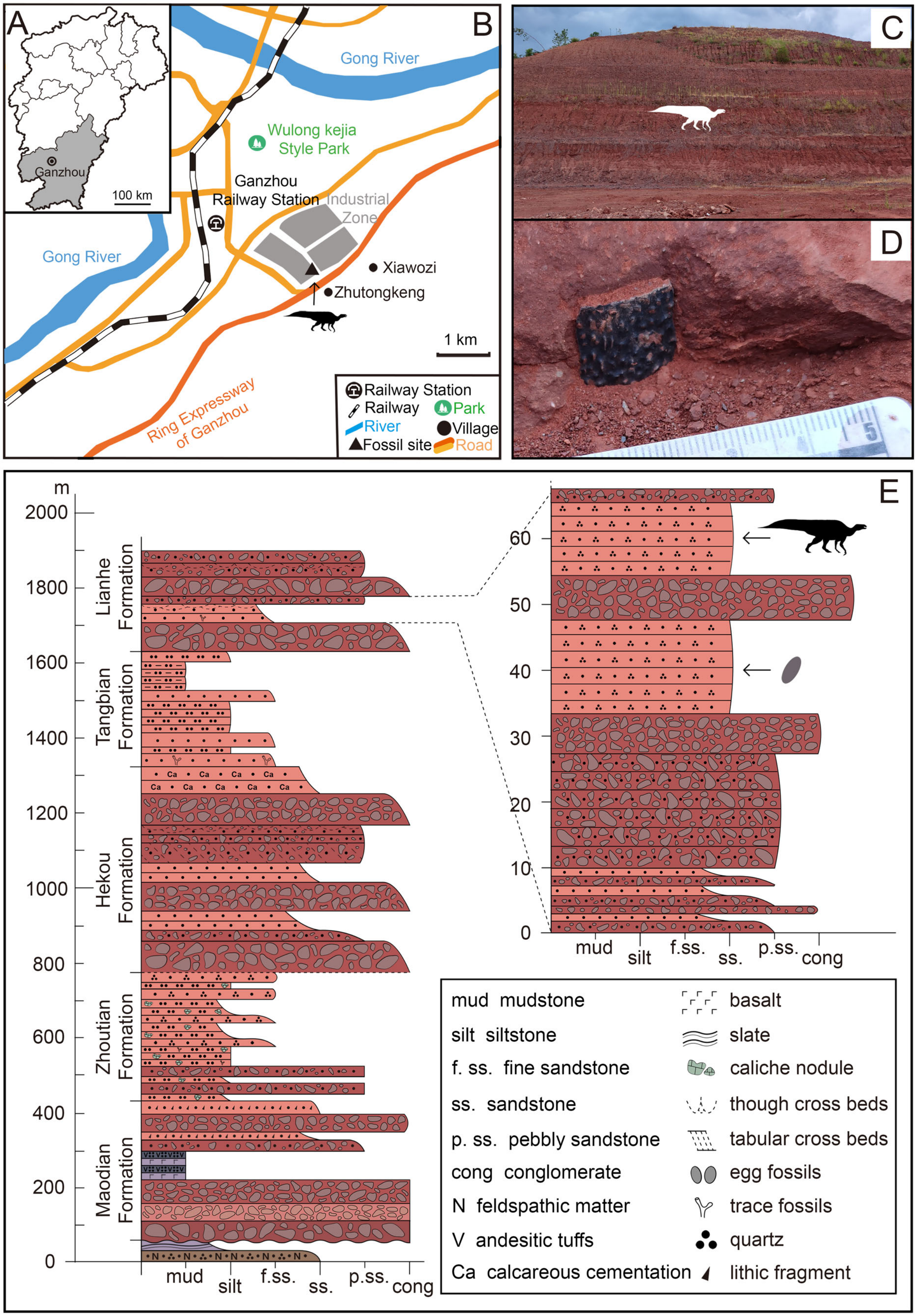
A
Ganzhou
100 km
B
Gong River
Wulong kejia Style Park
Ganzhou Railway Station
Industrial Zone
Gong River
Xiawozi
Zhutongkeng
1 km
Ring Expressway of Ganzhou
Railway Station
Railway
Park
River
Village
Fossil site
Road
C
D
E
m
2000
1800
1600
1400
1200
1000
800
600
400
200
0
Lianhe Formation
Tangbian Formation
Hekou Formation
Zhoutian Formation
Maodian Formation
Ca
N
V
mud
silt
f.ss.
ss.
p.ss.
cong
60
50
40
30
20
10
0
mud
silt
f.ss.
ss.
p.ss.
cong
mud mudstone
silt siltstone
f. ss. fine sandstone
ss. sandstone
p. ss. pebbly sandstone
cong conglomerate
N feldspathic matter
V andesitic tuffs
Ca calcareous cementation
basalt
slate
caliche nodule
though cross beds
tabular cross beds
egg fossils
trace fossils
quartz
lithic fragment

China; **BYU**, Brigham Young University Museum of Paleontology, Provo, USA; **CMN**, Canadian Museum of Nature, Ottawa, Canada; **CPC**, Colección Paleontológica de Coahuila (Paleontological Collection of Coahuila) Saltillo, Coahuila, Mexico; **GMH**, Geological Museum of Heilongjiang, Harbin, China; **HM**, Hobetsu Museum, Hobetsu area of Mukawa town, Japan; **IVPP**, Institute of Vertebrate Paleontology and Paleoanthropology, Chinese Academy of Sciences, Beijing, China; **JXGM**, Jiangxi Geological Museum, Nanchang, China; **LACM**, Natural History Museum of Los Angeles County, Los Angeles, USA; **MOR**, Museum of the Rockies, Bozeman, USA; **MPC**, Paleontological Center of the Mongolian Academy of Sciences, Ulaanbaatar, Mongolia; **ROM**, Royal Ontario Museum, Toronto, Canada; **TMP**, Royal Tyrrell Museum of Palaeontology, Drumheller, Canada; **USNM**, United States National Museum, Smithsonian Institution, Washington, DC, USA; **YPM**, Yale Peabody Museum of Natural History, New Haven, USA

Material and methods

Material identification and preparation

The specimens assigned to the new saurolophine were collected from a bonebed of brown sandstone within the middle of the Lianhe Formation, near the East China International Trade and Logistics Park of Ganzhou City. The specimens are now housed at the BGS-JX, where the fossil material was carefully prepared. All necessary permits were obtained from this institute for this study, which complied with all relevant regulations. The fossil material includes a partial skull containing two left jugals and one left quadrate, two maxillae, one left postorbital, one left nasal, two right and one left dentaries, a pair of surangulars, an incomplete posterior caudal series, and many largely disarticulated postcranial elements. The vast majority of the elements were partially exposed along two large blocks that could be pieced back together (Figs. 2, 3). No convincing taphonomic or osteological evidence was found to suggest that more than one hadrosauroid taxon, or other fossil reptiles, were present in this bonebed. As the Guifeng Group shows rapid accumulation of fluvial and alluvial depositions, the disarticulated condition of most bones appears to be attributed to hydraulic transportation over short distances after death and corpse decomposition (Chen et al., 2016; T. Li et al., 2017; Xiao et al., 2013).

All available specimens from the bonebed are likely to pertain to at least two individuals with slight size differences, for the following reasons: three sets of two duplicate bones (i.e. two left tibiae, two right dentaries and two left scapulae) were collected from the bonebed; the duplicate sets have similar size proportions to each other (e.g. the length ratio of ~0.82 between the coronoid processes of the two right dentaries, and the depth ratio of ~0.8 between the proximal ends of the two left tibiae); other elements are approximately proportionate in size when compared with published data on some nearly complete hadrosauroid skeletons. Osteological comparisons with other hadrosauroid taxa were made based on direct observations and relevant literature. The suggested taxonomic scheme of Hadrosauridae follows Prieto-Márquez (2010b), which generally matches the phylogenetic topology presented here.

Phylogenetic analysis

The systematic position of the new hadrosaurid taxon was assessed by parsimony analysis. The character matrix used here follows Dai et al. (2025), updated from H. Xing et al. (2017), and consists of 65 species-level taxa and 346 unordered characters (including 235 cranial characters and 111 postcranial characters). For the new taxon, 53 cranial characters and 22 postcranial characters were scored based on all available material from the bonebed. The updated data matrix was analysed using TNT version 1.6 (Goloboff & Morales, 2023). A maximum of 10,000 trees were retained in memory for the traditional heuristic search, which used a random seed of 1 and 1000 Wagner-tree replicates. Tree bisection and reconnection (TBR) was employed as the swapping algorithm, with 100 trees saved per replicate. The processing was terminated when it reached the maximum number of trees. Finally, a strict consensus was generated to summarize the phylogenetic interrelationships among hadrosauroids. Bootstrap support values were calculated using the standard ‘Resampling’ option with 100 replicates of absolute frequencies. Bremer decay indices were obtained via the ‘BREMER.RUN’ script.

Reconstruction of ancestral areas

In order to better assess the geographical origins and dispersal patterns of Saurolophinae and its major clades,

◄

Figure 1. Geographical and stratigraphical distribution of *Gongshuilong fanwei* gen. et sp. nov. in China. **A**, map showing the fossil locality in Ganzhou City, Jiangxi Province, China; **B**, map of the fossil site in Ganzhou City; **C**, geological cross section of the Lianhe Formation; **D**, eggshell fragments found beneath the fossil-bearing layer; **E**, stratigraphical column of the Lianhe Formation of Ganzhou Basin, showing the stratigraphical section of *Gongshuilong.*

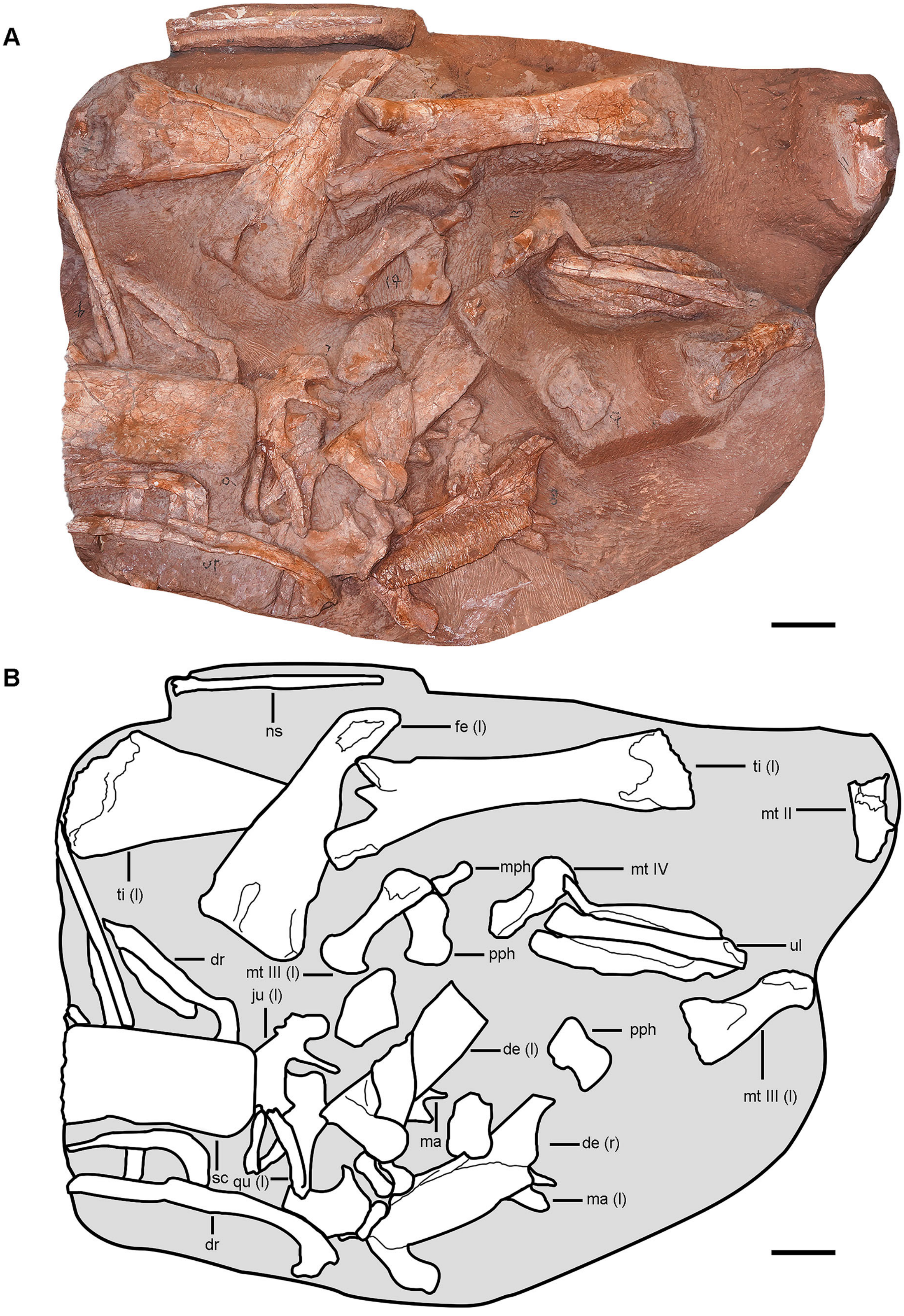
A
B
ns
fe (l)
ti (l)
ti (l)
mt II
mph
mt IV
dr
mt III (l)
pph
ul
ju (l)
de (l)
pph
mt III (l)
ma
de (r)
sc
qu (l)
ma (l)
dr

we performed biogeographical reconstruction using the Bayesian binary method (BBM) implemented in RASP version 4 (Yu et al., 2020). The quantitative BBM analysis with the topology of the strict consensus and biogeographical data was run with the setting of 50,000 cycles, 10 chains and sampling every 100 cycles. The temperature option was set at 0.1 and the model of state frequencies was chosen as a fixed JC (Jukes-Cantor model) one. The maximum number of ancestral areas for all nodes was set at five. After the calculations, the 'Single Area' model was selected and the independent probabilities of putative ancestral areas for each node was summarized and plotted as a pie chart.

Systematic palaeontology

Dinosauria Owen, 1842
Ornithischia Seeley, 1888
Ornithopoda Marsh, 1881
Iguanodontia Dollo, 1888 *sensu* Sereno, 1998
Hadrosauriformes Sereno, 1997 *sensu* Sereno, 1998
Hadrosauroidea Cope, 1869 *sensu* Sereno, 1998
Hadrosauridae Cope, 1870 *sensu* Sereno, 1998
Saurolophinae Brown, 1914 *sensu* Prieto-Márquez, 2010b
Gongshuilong gen. nov.

Type species. *Gongshuilong fanwei* sp. nov.

Etymology. 'Gongshui', pinyin of the Mandarin Chinese term meaning the Gong River, which is quite close to the fossil location; 'long', pinyin of the Mandarin Chinese term meaning the dragon.

Diagnosis. As for the type and only known species.

Gongshuilong fanwei sp. nov.
(Figs 2–6, 8)

Etymology. 'fanwei', pinyin of the Mandarin Chinese term that denotes the sail-like tail largely attributed to the extremely elongate, curved neural spines along the posterior caudal vertebrae.

Holotype. BGS-JX F001-1, a nearly complete right dentary.

Paratype. BGS-JX F001-2, a partial facial skeleton containing the left jugal and quadrate.

Referred material. All retrieved elements from the bonebed BGS-JX F001, except for the holotype and paratype. Particularly important material includes: BGS-JX F001-3, a left maxilla exposing only its anterior end; BGS-JX F001-4, a partial left nasal; BGS-JX F001-5, a left postorbital missing the anterior ramus; BGS-JX F001-6, a nearly complete left surangular; BGS-JX F001-7, a partial right surangular; BGS-JX F001-8, 9, 10 and 11, four cervical vertebrae; BGS-JX F001-12, a posterior dorsal vertebra missing the neural spine; BGS-JX F001-13, 10 articulated posterior caudal vertebrae; BGS-JX F001-14, a partial left tibia; BGS-JX F001-15, a left femur missing the proximal end; BGS-JX F001-16, a left scapula missing part of the distal blade; BGS-JX F001-17, a left scapula only preserving its proximal region; BGS-JX F001-18, a partial left coracoid; BGS-JX F001-19, a nearly complete left humerus; and BGS-JX F001-20, a right humerus exposing its proximal half.

Locality and horizon. The bonebed elements ascribed to *Gongshuilong* were collected from a quarry during the construction of the East China International Trade and Industrial Zone. The quarry is located at the Zhutongkeng locality, Shahe Town, Zhanggong District, Ganzhou City, Jiangxi Province, and is ~2 km southeast of the railway station (Fig. 1A, B). The horizon where the elements were retrieved is limited to the middle of the Maastrichtian Lianhe Formation (T. Li et al., 2017; Xi et al., 2021) and is mainly composed of ~3 m thick brown sandstone.

Diagnosis. Medium-sized saurolophine hadrosaurid (~7 m long in presumable adults) possessing the following unique combination of features (probable autapomorphy*): elevated anterodorsal process of the maxilla slightly longer than the anteroventral one (generally differing from the condition in non-hadrosaurid hadrosauroids and lambeosaurines); orbital margin of the jugal almost as wide as the infratemporal margin (differing from the condition in brachylophosaurins); dentary tooth crowns ornamented with a median primary ridge (generally differing from the condition in non-hadrosaurid hadrosauroids, and distinct from the condition in *Rhinorex*) and relatively small marginal denticles (generally differing from the condition in non-hadrosaurid hadrosauroids, and distinct from the condition in *Gryposaurus latidens* and *Aralosaurus*); extremely shortened edentulous margin of the dentary (generally differing from the condition in lambeosaurines and

◄

Figure 2. Skeletons of *Gongshuilong fanwei* gen. et sp. nov. in block 1 from the Zhanggong District, Ganzhou City (BGS-JX F001). **Abbreviations**: **de**, dentary; **dr**, dorsal rib; **fe**, femur; **ju**, jugal; **ma**, maxilla; **mph**, manual phalanx; **mt II**, metatarsal II; **mt III**, metatarsal III; **mt IV**, metatarsal IV; **ns**, neural spine; **pph**, pedal phalanx; **sc**, scapula; **ti**, tibia; **ul**, ulna. 'l' and 'r' indicate left and right. Scale bar = 15 cm.

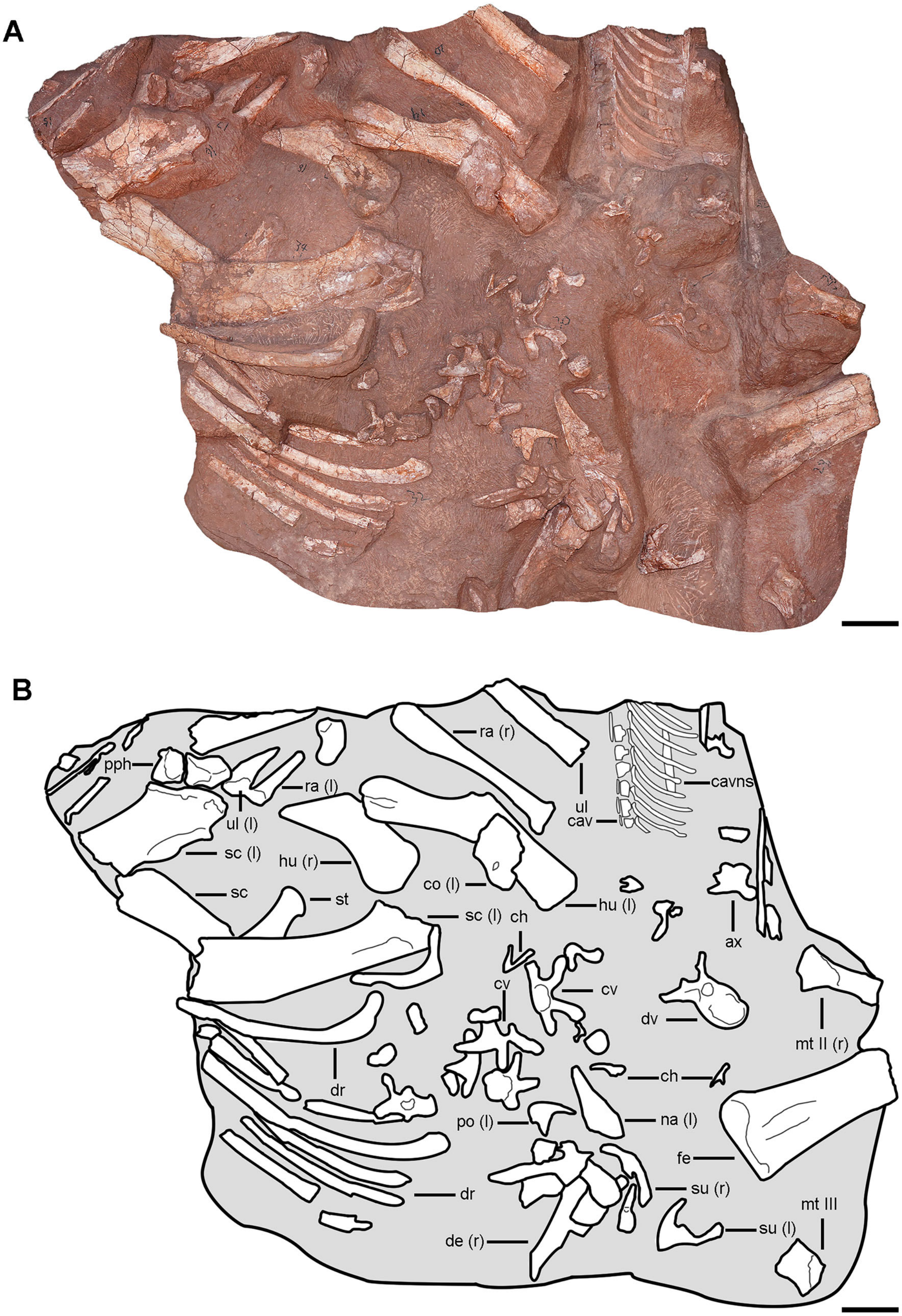
A
B
pph
ra (r)
ra (l)
ul (l)
ul
cav
cavns
sc (l)
hu (r)
co (l)
hu (l)
sc
st
sc (l)
ch
ax
cv
cv
dv
mt II (r)
dr
ch
po (l)
na (l)
fe
su (r)
dr
mt III
su (l)
de (r)

saurolophines); anterodorsally inclined long axis of the dentary tooth row relative to the posteroventral edge of the dentary ramus (generally differing from the condition in non-brachylophosaurin hadrosauroids); slightly dorsally curved retroarticular process of the surangular with a broadly arcuate posteroventral corner (generally differing from the condition in non-hadrosaurid hadrosauroids and lambeosaurines); anteroposteriorly wide, gradually tapering ventral process of the postorbital (generally differing from the condition in most hadrosaurids, but similar to the condition in *Shantungosaurus* and *Edmontosaurus*); shallowly arcuate quadratojugal notch located around the dorsoventral midpoint of the quadrate shaft (generally differing from the condition in non-hadrosaurid hadrosauroids and most saurolophines, but similar to the condition in *Acristavus* and *Maiasaura*); greatly elongate, moderately recurved, posterodorsally directed neural spines of the posterior caudal vertebrae that are ~8.5 times as tall as their corresponding centra*; scapula with an almost straight, anteriorly directed acromial process (generally differing from the condition in non-hadrosaurid hadrosauroids and lambeosaurines) and a poorly developed deltoid ridge (generally differing from the condition in saurolophines); and strongly mediolaterally constricted deltopectoral crest of the humerus relative to the distal neck (generally differing from the condition in lambeosaurines and non-brachylophosaurin saurolophines).

Description and comparisons

Skull and mandible

Maxilla. Two maxillae are preserved in the bonebed, and only the anterior ends of both bones are partially exposed (Fig. 2, Supplemental material Fig. S2D, S2E). The anterodorsal process of the maxilla is much more elevated than the anteroventral one, which is typical of Saurolophinae (Gates et al., 2011; Prieto-Márquez, 2010b). However, the anterodorsal process is slightly longer than the anteroventral one, as in *Eotrachodon* (Prieto-Márquez et al., 2016). This contrasts with many other saurolophines such as *Saurolophus* (e.g. MPC 100/706), *Brachylophosaurus* (e.g. MOR 794) and *Edmontosaurus* (e.g. CMN 2289), where the elongate anterodorsal process markedly exceeds the anteroventral one.

Nasal. A partial left nasal is taphonomically exposed in medial view, leaving the posterior part of the anterodorsal process and most of the posterior plate (Fig. 3, Supplemental material Fig. S2A). Although incomplete, the posterior part is dorsoventrally deeper than mediolaterally wide, and shows a large, laterodorsally convex side that serves as the posterior region of the circumnarial fossa. This is very similar to the condition in all saurolophines except saurolophins, including *Laiyangosaurus* (Zhang et al., 2019) and *Probrachylophosaurus* (Freedman Fowler & Horner, 2015).

Jugal. Two incomplete jugals were identified from the bonebed. Each element is triradiate in lateral or medial outline (Fig. 4B, C). It is anteroposteriorly elongate with a shallow, slightly concave ventral margin, as in most early-branching hadrosauroids (Prieto-Márquez, 2011; Tsogtbaatar et al., 2019; You et al., 2003) and some saurolophines such as *Kritosaurus* (e.g. USNM 8629) and *Prosaurolophus* (e.g. ROM 787), but unlike the deeply concave ventral edge seen in most brachylophosaurins and edmontosaurins including *Acristavus* (MOR 1155) and *Kerberosaurus* (e.g. AENM 2/921-2). The anterior process of the jugal has a deep posterodorsal region and a wide, sub-triangular posteroventral corner, very similar to the condition in *Maiasaura* (e.g. ROM 44770) and *Rhinorex* (BYU 13528). The rod-like, posteriorly tilted postorbital process separates the U-shaped ventral margins of the orbit and infratemporal fenestra. The orbital margin is almost as wide as the infratemporal margin, which differs from the wider orbital margin observed in all other brachylophosaurins, including *Wulagasaurus* (GMH 166). The posteroventral flange and posterodorsal process are either incompletely preserved or taphonomically concealed by other elements. In medial view, a nearly vertical crescent-shaped contact surface for the palatine occurs along the posterodorsal edge of the anterior process, which is also known from many hadrosaurids (H. Xing et al., 2017).

Postorbital. The left postorbital is partially preserved, with the missing anteromedial process and the lower half of the ventral process, and is moderately deformed by transverse matrix compression (Fig. 3, Supplemental material Fig. S2B, S2C). The preserved region of the ventral process is proportionally anteroposteriorly wider than that in all hadrosaurids except *Shantungosaurus* and *Edmontosaurus* (Xing, Zhao et al., 2014). However,

Figure 3. Skeletons of *Gongshuilong fanwei* gen. et sp. nov. in block 2 from the Zhanggong District, Ganzhou City (BGS-JX F001). **Abbreviations**: **ax**, axial cervical; **cav**, caudal vertebra; **cavns**, caudal vertebra neural arch; **ch**, chevron; **co**, coracoid; **cv**, cervical vertebra; **de**, dentary; **dr**, dorsal rib; **dv**, dorsal vertebra; **fe**, femur; **hu**, humerus; **mt II**, metatarsal II; **mt III**, metatarsal III; **na**, nasal; **po**, postorbital; **pph**, pedal phalanx; **ra**, radius; **sc**, scapula; **st**, sternum; **su**, surangular; **ul**, ulna. ‘l’ and ‘r’ indicate left and right. Scale bar = 15 cm.

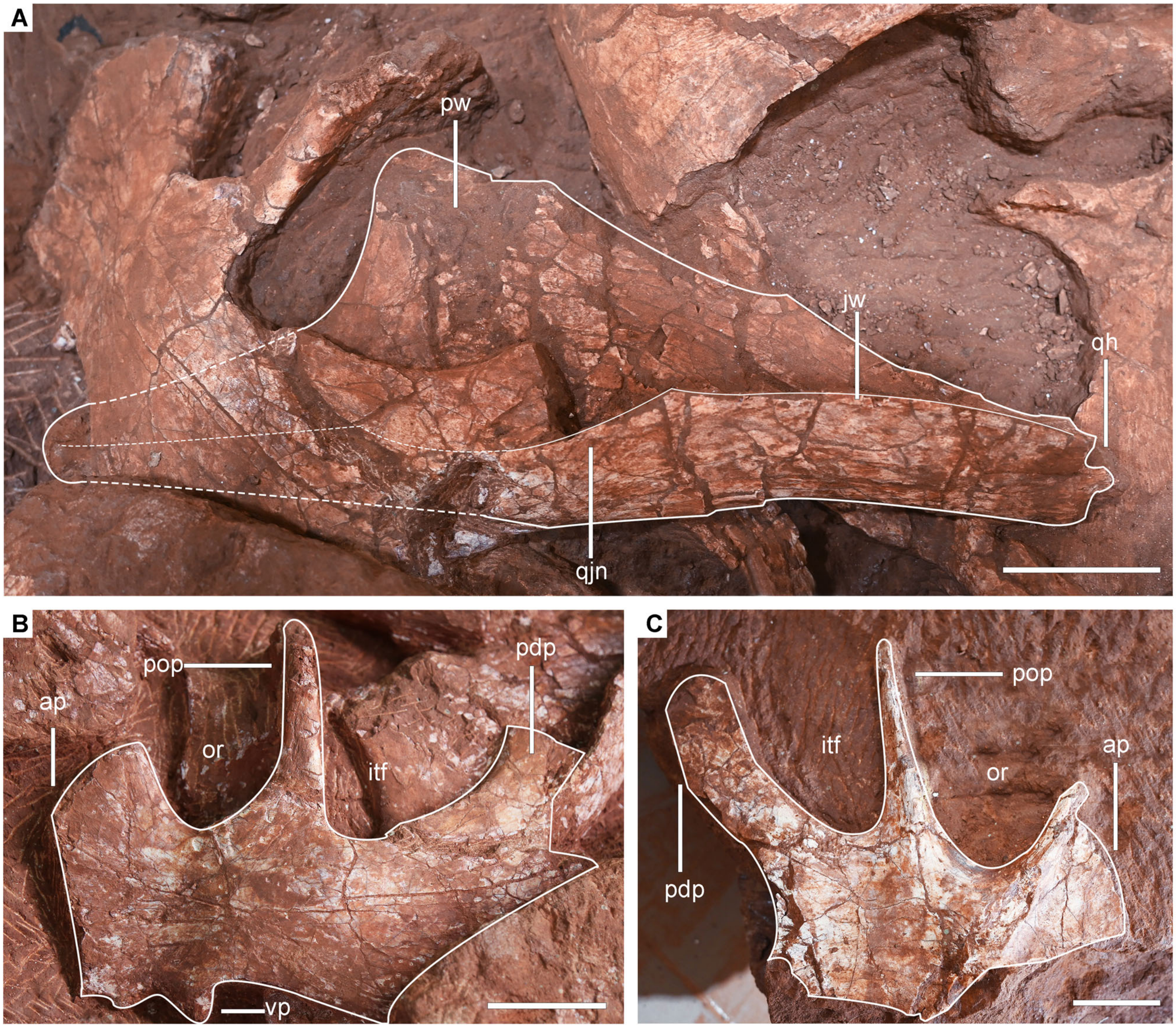

Figure 4. Facial elements of *Gongshuilong fanwei* gen. et sp. nov. **A**, left quadrate in lateral view (BGS-JX F001-2); **B**, left jugal in lateral view (BGS-JX F001-2); **C**, left jugal in medial view (BGS-JX F001-21). **Abbreviations**: **ap**, anterior process; **itf**, infratemporal margin; **jw**, jugal wing; **or**, orbital margin; **pdp**, posterodorsal process; **pop**, postorbital process; **pw**, pterygoid wing; **qh**, quadrate head; **qjn**, quadratojugal notch; **vp**, ventral spur. Scale bar = 5 cm.

unlike the condition in *Edmontosaurus* (e.g. AMNH 5730), the main body of the ventral process is not strongly swollen mediolaterally to form a large internal pocket (H. Xing et al., 2017).

Quadrate. The left quadrate is laterally exposed along the bonebed, and most of its ventral half is obscured by the posterior portion of the associated left jugal (Fig. 4A). The main shaft of the bone is nearly straight, in striking contrast to the strongly posteriorly curved condition in lambeosaurines such as *Velafrons* (CPC 59), *Tsintaosaurus* (e.g. IVPP V725) and *Parasaurolophus* (e.g. ROM 768). As in *Acristavus* (MOR 1155) and *Maiasaura* (e.g. YPM PU22405), the quadratojugal notch appears to be widely arched and anteroposteriorly shallow, located half-way up the bone. However, the equivalent is positioned well below half the dorsoventral height of the quadrate in many other saurolophines, including *Prosaurolophus* (e.g. ROM 1928), *Saurolophus* (e.g. CMN 8796), *Kerberosaurus*

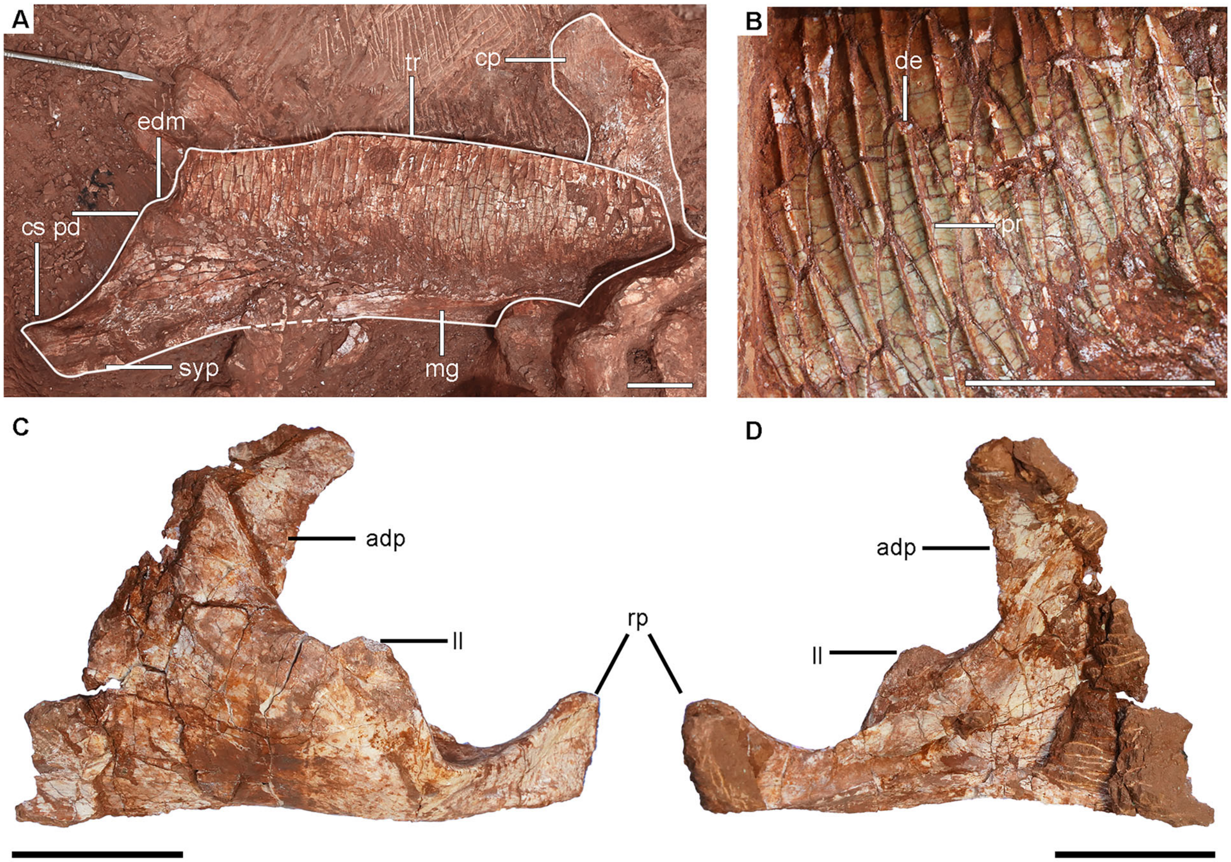

Figure 5. Lower jaw of *Gongshuilong fanwei* gen. et sp. nov. **A**, right dentary in lingual view (BGS-JX F001-1); **B**, dentary teeth in lingual view; **C**, left surangular in lateral view (BGS-JX F001-6); **D**, left surangular in medial view (BGS-JX F001-6). **Abbreviations**: **adp**, anterodorsal process; **cp**, coronoid process; **cs pd**, contact surface for predentary; **de**, denticle; **edm**, edentulous margin; **ll**, lateral lip; **mg**, Meckelian groove; **pr**, primary ridge; **rp**, retroarticular process; **syp**, symphysis; **tr**, tooth row. Scale bar = 5 cm.

(AENM 2/921-3) and *Probrachylophosaurus* (MOR 2919). Unlike the condition in most brachylophosaurins and kritosaurins, the squamosal buttress along the posterior margin of the dorsal quadrate is absent (Prieto-Márquez, 2010b). The pterygoid wing forms a wide, fan-shaped flange that slopes at approximately 45° with the main shaft.

Dentary. The right dentary BGS-JX F001-1 is well preserved, and its posteroventral part is obscured by some unidentified chunks of bones (Fig. 5A). As in other brachylophosaurins, the long axis of the dentary tooth row is anterodorsally inclined relative to the posteroventral edge of the dentary ramus (H. Xing et al., 2017). The dentary ramus is proportionally deeper than that in *Wulagasaurus* (GMH W184). The bone has an extremely shortened edentulous margin between the predentary facet and tooth row, with the ratio of ~0.05 between the lengths of the margin and tooth row. This is very similar to the condition in many non-hadrosaurid hadrosauroids and *Velafrons* (Gates et al., 2007; Prieto-Márquez et al., 2016; Prieto-Márquez & Norell, 2010; Tsogtbaatar et al., 2019; X. Wang & Xu, 2001; You et al., 2003), but is distinct from the longer diastema in other saurolophids (Prieto-Márquez, 2010b). Although some saurolophids also possess relatively short edentulous margins, the ratio in those taxa ranges from 0.27 to 0.63, far exceeding the markedly low value of 0.05 observed here (Prieto-Márquez, 2008). In medial view, the dentary symphysis is slightly ventrally inclined, with the deflection angle of ~23°. This ventral deflection occurs slightly anterior to the mid-length of the tooth row. The Meckelian groove is situated at the posteroventral corner of the dentary ramus, wedging anteriorly along the ventromedial border of the posterior part of the bone. It tapers anteriorly and terminates around the anteroposterior midpoint of the ventromedial margin of the dentary ramus. As in most saurolophids, the coronoid process is moderately inclined anteriorly (Godefroit et al., 2000; Horner, 1983). The ovate apex of the coronoid process is anteroposteriorly expanded with a more convex anterior margin, as in many lambeosaurines and most brachylophosaurins (Cuthbertson & Holmes, 2010; Freedman Fowler & Horner, 2015; Godefroit et al., 2000, 2012). In *Gongshuilong*, a thick dorsoventrally oriented ridge occurs along the posterior margin of the medial side of the coronoid process.

Surangular. One left and one right surangular of similar size were recovered from the same bonebed block, and were found in close proximity to each other (Fig. 3). The left surangular is nearly complete, exhibiting a tall anterodorsal process, an elevated lateral lip and a nearly straight retroarticular process that extends posteriorly (Fig. 5C, D). In ventral view, the bone is medially curved, with a narrow contact surface for the angular. The surangular resembles that of other saurolophines in possessing a slightly dorsally curved retroarticular process that has a broadly arcuate posteroventral corner. This contrasts with the strongly upward curvature of the process with a nearly right-angled posteroventral edge seen in most lambeosaurines, such as *Lambeosaurus* (e.g. CMN 2869) and *Amurosaurus* (e.g. GMH WH190). As in other saurolophids (Evans & Reisz, 2007; Godefroit, Bolotsky et al., 2004; Prieto-Márquez, 2005), no surangular foramen is present on the lateral surface of the lateral lip.

Dentition. Only information on the dentary tooth battery is available: ∼40 tooth positions can be counted from the well-preserved right dentary (i.e. BGS-JX F001-1). There are four to six teeth per alveolus along the entire dentary, reaching the maximum number in the middle of the tooth battery. Although the occlusal surface of the tooth battery is transversely distorted and closely appressed to the matrix, the number of functional teeth per alveolus can still be determined through careful observation and palpation: two functional teeth along the anterior and posterior ends, and three functional ones in the middle. This combination pattern of the dentary occlusal surface is also seen in other brachylophosaurins and most kritosaurins (Prieto-Márquez, 2012; H. Xing et al., 2017). The height/width ratio of each complete tooth crown ranges from 2.8 to 3.2. A median primary ridge serves as the single ornament along the enamelled lingual surface of each tooth crown (Fig. 5B), as in most saurolophines including *Brachylophosaurus* (e.g. CMN 8893) and *Kamuysaurus* (HMG 1219). In lingual view, each primary ridge is either straight or slightly sinuous, and the tooth crowns do not overlap one another. There is a series of relatively small denticles along the dorsal half of the margin of each tooth crown, very similar to the condition in all saurolophines except *Gryposaurus latidens* (H. Xing, Wang et al., 2014).

Postcranium

Cervical vertebra. One nearly complete cervical vertebra is visible, along with three isolated neural arches distributed nearby (Fig. 6A). The centrum is opisthocoelous and transversely wider than dorsoventrally deep, as in most other hadrosauroids (Horner et al., 2004; Norman, 2004). The neural canal is elliptical in anterior view, and its width is twice the height. The parapophysis is obscured due to the poorly preserved condition. Each rod-like diapophysis extends laterally to form the central support for the oval articular surface of the truncated prezygapophysis. The paired postzygapophyses are elongate and curved posterolaterally and dorsally, forming an angle of ∼90° in dorsal view.

Dorsal vertebra. One dorsal vertebra is poorly preserved, lacking the entire neural spine (Fig. 6B). The centrum appears to be amphiplatyan. It is oval in anterior view, slightly dorsoventrally deeper than transversely wide. The neural canal is roughly round between the bases of the paired neural arches. The prezygapophysis faces dorsomedially, forming an angle of 45° with the horizontal. The diapophysis projects dorsolaterally, and is angled ∼100° from its counterpart.

Caudal vertebra. Ten articulated posterior caudal vertebrae are partially exposed along the bonebed, and are visible in left lateral view (Fig. 6C). The lateral outlines of the centra are sub-rectangular and they are anteroposteriorly much longer than dorsoventrally tall, with no evidence of transverse processes along the incomplete caudal series. Between the simplified prezygapophyseal and postzygapophyseal facets of each caudal, the neural arches markedly extend and converge posterodorsally to form a greatly elongate, moderately recurved neural spine, somewhat similar to the condition in *Magnapaulia* (LACM 20873). The neural spines of the partial posterior caudal series are ∼8.5 times as tall as their corresponding centra. Therefore, *Gongshuilong* exhibits substantially higher neural spines along the posterior caudal series, compared with other iguanodontians (Fig. 7). The box plot of the height ratios between the neural spines and centra of the preserved posterior caudal series exhibits a much higher interval of values for *Gongshuilong*, compared to other iguanodontians with available data for the posterior caudals, where the ratios are typically less than 4 (Fig. 7). This reflects a still

Figure 6. Cervical, dorsal and caudal vertebrae of *Gongshuilong fanwei* gen. et sp. nov. **A**, cervical vertebrae in posterior and anterior view (BGS-JX F001-8, 9 and 10); **B**, dorsal vertebra in anterior view (BGS-JX F001-12); **C**, caudal vertebra serials with articulated neural spines in left lateral view (BGS-JX F001-13). **Abbreviations**: **cav**, caudal vertebra; **ch**, chevron; **di**, diapophysis; **nc**, neural canal; **ns**, neural spine; **poz**, postzygapophysis; **pre**, prezygapophyses. Scale bar = 5 cm.

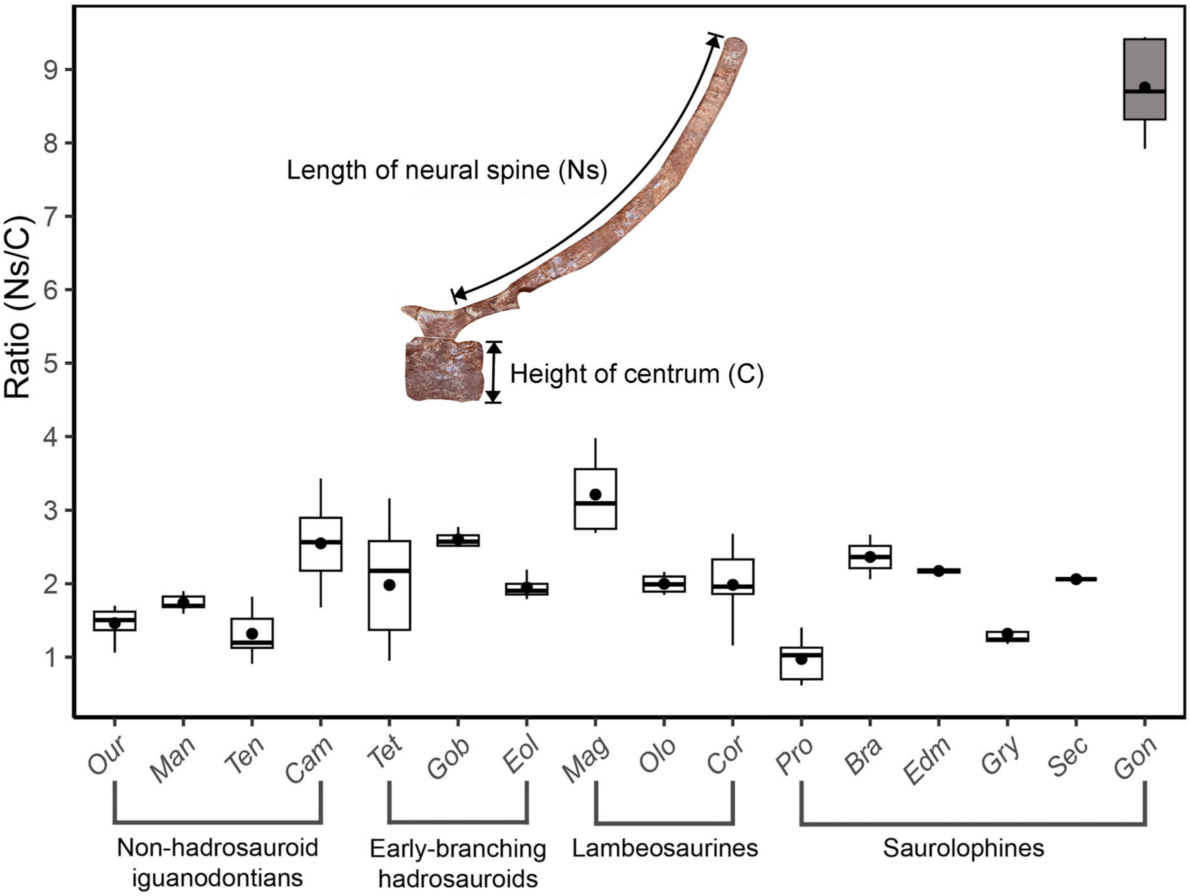

Figure 7. Box plot showing the distribution of the ratio between the length of the available neural spines from the posterior caudal vertebrae and the height of the corresponding centra across different taxa (see Supplemental material Table S2 for detailed measurements). Each box represents the interquartile range (IQR), with the horizontal line indicating the median and the black dot indicating the mean. **Abbreviations**: **Bra**, *Brachylophosaurus canadensis*; **Cam**, *Camptosaurus aphanoecetes*; **Cor**, *Corythosaurus casuarius*; **Edm**, *Edmontosaurus regalis*; **Eol**, *Eolambia caroljonesa*; **Gob**, *Gobihadros mongoliensis*; **Gon**, *Gongshuilong fanwei*; **Gry**, *Gryposaurus notabilis*; **Mag**, *Magnapaulia laticaudus*; **Man**, *Mantellisaurus atherfieldensis*; **Olo**, *Olorotitan arharensis*; **Our**, *Ouranosaurus nigeriensis*; **Pro**, *Probrachylophosaurus bergei*; **Sec**, *Secernosaurus koerneri*; **Ten**, *Tenontosaurus tilletti*; **Tet**, *Tethyshadros insularis.*

fairly high posterior part of the *Gongshuilong* tail beyond our previous thoughts on iguanodontian body plans (Fig. 7).

Dorsal rib. Some dorsal ribs are incompletely preserved along the bonebed (Fig. 3), featuring an elongate, slightly curved shaft with a large capitulum that does not differ significantly from that of other hadrosaurids. The shaft is anteroposteriorly flattened, and bears a slightly convex anterior side and a gently concave posterior side.

Scapula. Two partial left scapulae and the distal third of a scapular blade with uncertain body side are known from the bonebed, and the two left ones are just exposed in lateral outline (Fig. 8A, B). The dorsal margin of the scapula is slightly convex and arched distally, in striking contrast to the nearly straight dorsal margin seen in some early-branching hadrosauroids such as *Eolambia* (e.g. CEUM 52097) and *Gilmoreosaurus* (e.g. AMNH 6551). The bone has a nearly straight, anteriorly directed acromial process, a relatively wide proximal neck and the slightly distally divergent dorsal and ventral margins of the distal blade, which are all common among saurolophines but rarely reported in lambeosaurines (Dilkes, 1999; Gates & Sampson, 2007; Prieto-Márquez, 2010b; Prieto-Márquez & Guenther, 2018). However, the lateral side of the proximal scapula is not defined by a prominent deltoid ridge, a character typical of Saurolophinae

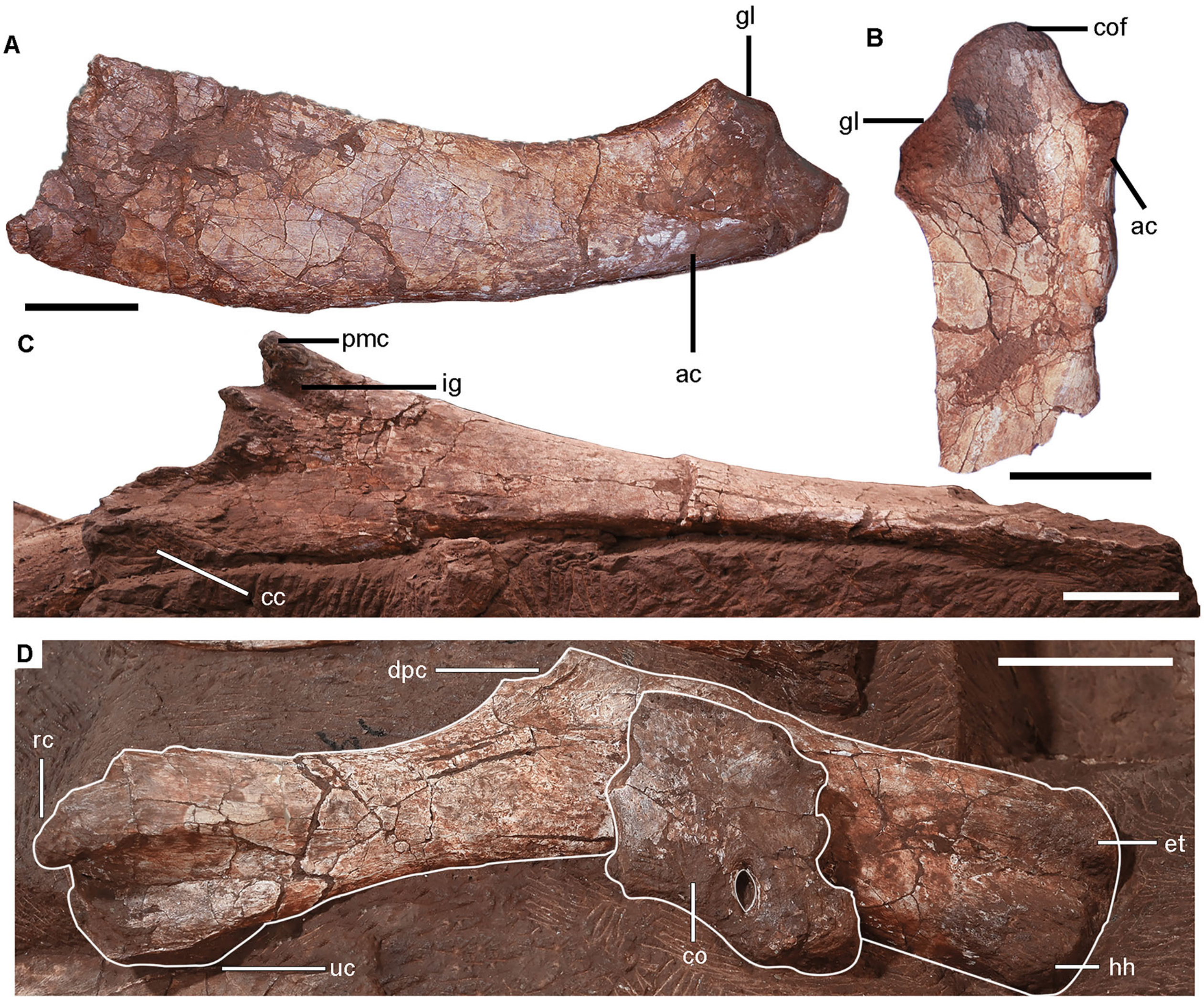

Figure 8. Partial appendicular bones of *Gongshuilong fanwei* gen. et sp. nov. **A**, left scapula in lateral view (BGS-JX F001-16); **B**, partially preserved left scapula in lateral view (BGS-JX F001-17); **C**, left tibia in lateral view (BGS-JX F001-14); **D**, left humerus in posterior view (BGS-JX F001-19) and left coracoid in lateral view (BGS-JX F001-18). **Abbreviations**: **ac**, acromial process; **cc**, cnemial crest; **co**, coracoid; **cof**, coracoid facet; **dpc**, deltopectoral crest; **et**, external tuberosity; **gl**, glenoid facet; **hh**, humeral head; **ig**, intercondylar groove; **pmc**, posteromedial condyle; **rc**, radial condyle; **uc**, ulna condyle. Scale bar = 10 cm.

(Prieto-Márquez & Wagner, 2009). This incipiently developed deltoid ridge is actually shared with many lambeosaurines, such as *Hypacrosaurus* (e.g. CMN 8501) and *Lambeosaurus* (e.g. TMP 82.38.01). In *Gongshuilong*, the proximal end of the scapula is mediolaterally expanded to form the coracoid facet and the more ventrally positioned glenoid. The glenoid is deeply concave and generally as long as the coracoid facet. Proximolaterally, a U-shaped shallow fossa occurs between the nearly straight acromial process and the posteroventral corner of the glenoid. As in other hadrosauroids, the distal blade is mediolaterally compressed and sub-rectangular.

Coracoid. A partial left coracoid was found in close proximity to the left humerus (Fig. 8D). The coracoid is reduced in size relative to the scapula. The coracoid foramen is oval in shape. A relatively large biceps tubercle projects laterally from the anterolateral surface of the coracoid, consistent with the condition observed in other saurolophids (Prieto-Márquez, 2010b).

Humerus. Two humeri are visible from the bonebed; the right humerus is distally embedded into the matrix, and the left one is nearly complete and fully exposed (Figs. 3, 8D). The humerus has a mediolaterally broad proximal end that consists of the external and internal tuberosities and the humeral head, as well as a slightly twisted distal end containing the ulnar and radial condyles. This bone is relatively gracile in posterior view, with an anterolaterally projecting deltopectoral crest along its proximal half. The deltopectoral crest is proximodistally elongate, and accounts for 59% of the total length of the humerus; this condition is also observed in some saurolophids, such as *Corythosaurus*, *Olorotitan*, *Shantungosaurus* and *Saurolophus* (Dilkes, 1999; Godefroit et al., 2012; Maryańska & Osmólska, 1984; Takasaki et al., 2023; H. Xing, Zhao et al., 2014). Nevertheless, the deltopectoral crest in *Gongshuilong* exhibits a relatively weak mediolateral expansion, and the width ratio between the midshaft at the distal third of the deltopectoral crest and distal neck is ~1.46. This transverse constriction of the deltopectoral crest is also reported in many non-hadrosaurid hadrosauroids and other brachylophosaurins (Godefroit et al., 2008; McDonald et al., 2012; Prieto-Márquez & Wagner, 2009; Tsogtbaatar et al., 2019; H. Xing et al., 2012). Distally, the medial ulnar and lateral radial condyles are separated by a deep intercondylar sulcus.

Ulna. In available ulnas, only part of the midshaft is preserved and partially exposed (Fig. 3). This bone is obviously more robust than the radius. The proximal region of the ulna is much more mediolaterally expanded than the rest of the bone.

Radius. A nearly complete right radius is fully exposed along the bonebed (Fig. 3). The bone is almost un-bent and rod-shaped, with a ratio of ~5.9 between the total length and maximum width of the proximal head. It does not differ significantly from that of other hadrosaurids. The proximal head flares more medially than laterally, and has a slightly convex, sub-oval articular surface for the lateral condyle of the humerus. By contrast, the distal third of the radius is more expanded mediolaterally and anteroposteriorly than the proximal head.

Femur. Two incomplete femurs are preserved. However, the distal ends of both femora remain intact (Figs 2, 3). Each distal femur displays enlarged lateral and medial condyles, although they are heavily damaged. The condyles are fused together to form a partially enclosed anterior intercondylar tunnel.

Tibia. Two tibiae are partially preserved and moderately distorted (Figs. 2, 8C). The best-preserved tibia is fully exposed, but its proximal and distal ends are broken. The bone shows few discrepancies with that in other hadrosaurids. The shaft is expanded anteroposteriorly along its proximal part and mediolaterally along its distal part, and is medially twisted along its proximal half, forming a rotation angle of ~90° in distal view. Proximally, the wing-like cnemial crest appears to be much more prominent than the lateral and posteromedial condyles. In lateral view, the two condyles are entirely separated by a deep longitudinal intercondylar groove.

Metatarsals. Two metatarsals II, three metatarsals III and one metatarsal IV are poorly preserved in the bonebed (Figs. 2, 3). Metatarsal III is the largest element of the series, with the mediolaterally expanded proximal and distal ends and the gradually constricted midshaft. As in other hadrosauroids, the proximal part of metatarsal III is deeply concave medially but moderately convex laterally. Metatarsals II and IV are slightly shorter than metatarsal III, but are similar to each other in total length. Metatarsal II is more compressed mediolaterally than metatarsal IV, and gently curves medially along its distal third. By contrast, metatarsal IV displays a strongly lateral curvature and a slight mediolateral constriction along its distal half.

Phylogenetic results

The current phylogenetic analysis produced 18 most parsimonious trees (MPTs) of 1100 steps in tree length, each with a consistency index of 0.449 and a retention index of 0.848. The strict consensus shown in Figure 9 reveals a suggested taxonomic framework of Hadrosauridae, namely the earliest diverging hadrosaurid *Hadrosaurus foulkii*, Saurolophinae and Lambeosaurinae, which is also argued by Prieto-Márquez (2010b). Within the strict consensus, Saurolophinae is represented by the clade of Brachylophosaurini + (Kritosaurini + (Edmontosaurini + Saurolophini)). All the saurolophine subclades, namely Brachylophosaurini by Gates et al. (2011); Kritosaurini by Lapparent and Lavocat (1955) and Prieto-Márquez (2014); Edmontosaurini by Brett-Surman (1989); and Saurolophini by Prieto-Márquez et al. (2015), exhibit their own phylogenetic topologies that generally follow the published definitions. The tribe Brachylophosaurini is posited as the earliest branching subclade of Saurolophinae. At the base of Brachylophosaurini, there is an unresolved polytomy constituted by *Wulagasaurus*, *Gongshuilong*, *Acristavus* and the clade of *Maiasaura* + (*Probrachylophosaurus* + *Brachylophosaurus*). Node support for the polytomy is moderate, with a bootstrap proportion of 48% and a Bremer decay index of 1. Therefore, *Gongshuilong fanwei* is recovered as one of

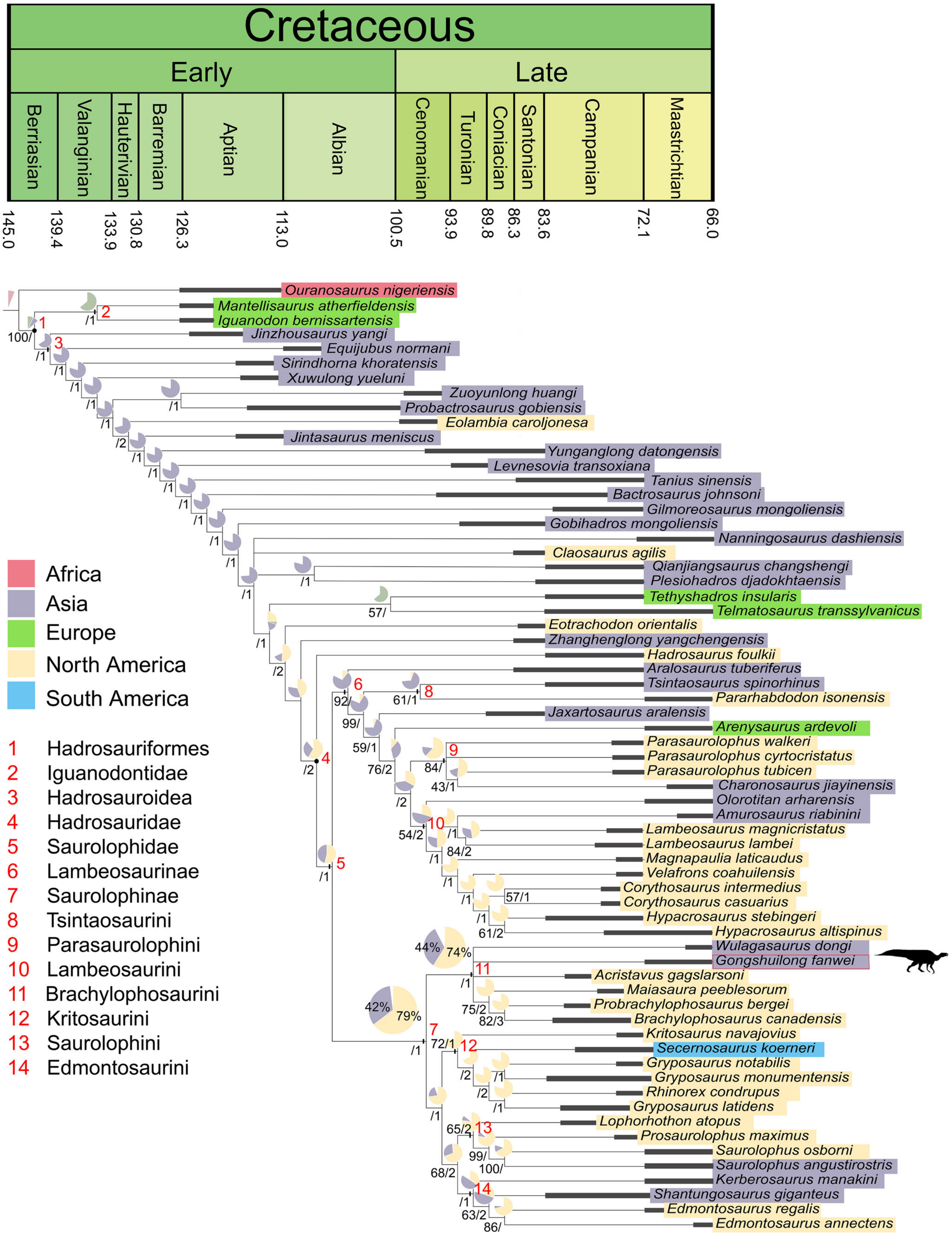

Figure 9. Time-calibrated strict consensus of the 18 most parsimonious trees from the parsimony analysis showing bootstrap proportions and Bremer support values (values are given as bootstrap proportion/Bremer support). Independent probabilities of biogeographical inferences for ancestral areas are shown as a pie chart at each internal node.

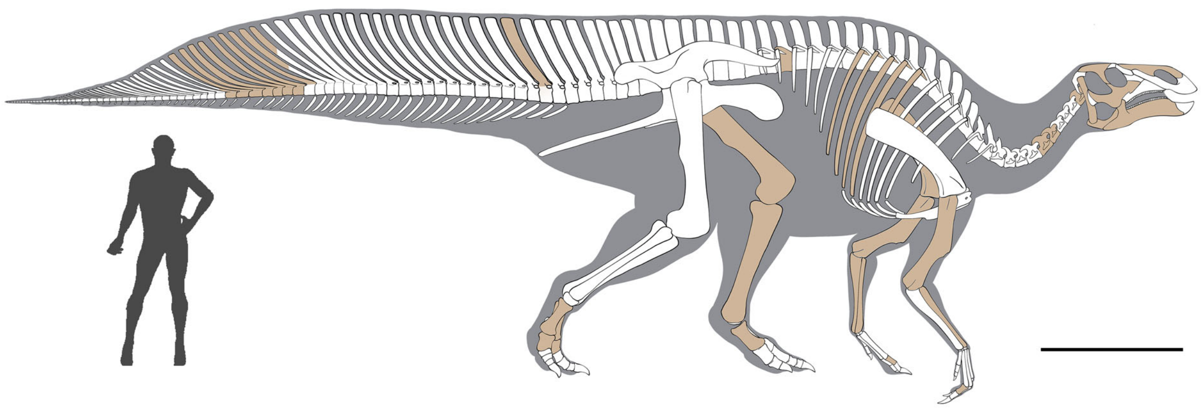

Figure 10. Skeletal restoration of *Gongshuilong fanwei* gen. et sp. nov. Scale bar = 1 m.

the earliest branching taxa within Brachylophosaurini, as it lies in an unresolved polytomy. In the current tree topology, all brachylophosaurin members are united by the following synapomorphies: characters 22(1), 75(1), 109(1), 144(1), 148(0), 150(1), 157(0), 216(1), 219(2), 232(0), 237(1) and 270(0) (see Supplemental material). *Gongshuilong fanwei* also presents two identifiable synapomorphies shared with other saurolophines: character 63(0), the absence of the strong upward curvature of the surangular retroarticular process; and character 263(2), the almost straight, anteriorly directed acromial process of the scapula.

Biogeographical results

The BBM analysis recovered North America and Asia as the potential ancestral areas of Hadrosauridae and its major subclades (Fig. 9, Supplemental material Fig. S4 and Table S3). The result of this biogeographical analysis indicates two relatively high independent probabilities of putative ancestral areas for Hadrosauridae, namely ∼0.69 for North America and ∼0.42 for Asia. Similarly, possible ancestral areas of Saurolophinae inferred by the BBM analysis are limited to the following two continents with higher probabilities: ∼0.79 for North America and ∼0.42 for Asia. By contrast, the Asian origin of Lambeosaurinae was regarded as predominant after the analysis, which yielded a particularly high independent probability of ∼0.86. For Saurolophidae, North America and Asia were recovered as two optimal ancestral areas, with relatively high independent probabilities of ∼0.65 and ∼0.61, respectively. The clade representing Brachylophosaurini was inferred to have originated from either North America or Asia; the probability of its Asian origin is ∼0.44, whereas the probability of a North American origin reaches ∼0.74. In the scenario on the Asian origin of Brachylophosaurini, one or two dispersal events from Asia to North America are postulated to have occurred, and subsequent vicariance events are very likely to have led to allopatric speciation in North America. For the scenario of the North American origin, two dispersal events from North America to Asia are expected to have occurred, with allopatric speciation caused by vicariance.

Discussion

Systematic position of *Gongshuilong fanwei*

Gongshuilong fanwei, represented by a series of largely disarticulated bone elements from the Zhutongkeng locality of Ganzhou City, exhibits a set of salient apomorphic features that are typical of saurolophines but distinct from the condition in lambeosaurines. These include an elevated anterodorsal process of the maxilla that exceeds the anteriormost end of the anteroventral one, a slightly dorsally curved retroarticular process of the surangular having a broadly arcuate posteroventral corner, the enamelled lingual side of each dentary tooth crown ornamented exclusively with a median primary ridge, and an almost straight, anteriorly directed acromial process of the scapula (Cuthbertson & Holmes, 2010; Dilkes, 1999; Gates et al., 2011; Gates &

Sampson, 2007; Prieto-Márquez, 2010b; H. Xing et al., 2017; H. Xing, Zhao et al., 2014). Therefore, the presence of these features strongly indicates a close affinity of this new taxon with Saurolophinae.

Furthermore, *Gongshuilong fanwei* possesses some meaningful traits common among brachylophosaurins but rarely observed in other saurolophines, including the primary ridge of each dentary tooth crown either straight or slightly sinuous, an anterodorsally inclined long axis of the dentary tooth row relative to the posteroventral margin of the dentary ramus, the anteroposteriorly expanded apex of the coronoid process with a more pronounced anterior region, and the strongly mediolaterally constricted deltopectoral crest of the humerus relative to the distal neck (quantitatively identified as a width ratio of less than 1.65 between the humeral midshaft across the maximum extent of the crest and the distal neck) (Godefroit et al., 2008; Prieto-Márquez, 2010b; H. Xing et al., 2012, 2017). The combination of these traits, together with the above-mentioned features typical of saurolophines, indirectly points to the possibility that *G. fanwei* represents a brachylophosaurin saurolophine.

Interestingly, *Gongshuilong fanwei* also displays several plesiomorphic characters that are mainly present in non-saurolophine hadrosauroids, such as a poorly developed deltoid ridge along the lateral side of the proximal scapula (shared with many early-branching hadrosauroids and most lambeosaurines), and an extremely shortened edentulous region of the dentary (shared with most early-branching hadrosauroids) (Gates et al., 2007; Prieto-Márquez and Norell 2010; Prieto-Márquez et al., 2016; Tsogtbaatar et al., 2019; X. Wang & Xu, 2001; You et al., 2003). The combination of such plesiomorphic and apomorphic features in some specific bones (e.g. the dentary, humerus and scapula) of *G. fanwei* reveals a pattern of mosaic evolution from non-hadrosaurid hadrosauroids to saurolophine hadrosaurids.

In addition to the features typical of Saurolophinae, common among brachylophosaurins but rarely reported in other saurolophines, and mainly shared with non-saurolophine hadrosauroids, *Gongshuilong fanwei* is likewise characterized by a distinctive autapomorphy, namely the extraordinarily elongate, moderately recurved, posterodorsally directed neural spines along the posterior caudal vertebrae. The elongation of neural spines is well documented in the dorsal and anterior caudal series of some hadrosaurids (e.g. *Barsboldia sicinskii*, *Hypacrosaurus altispinus*, *Magnapaulia laticaudus*), as well as the dorsal series of iguanodontian *Ouranosaurus nigeriensis*, but no previous work recorded comparable elongation along the posterior caudal series (Bertozzo et al., 2017; Brown, 1913; Maryanska & Osmólska, 1981; Prieto-Márquez et al., 2012). In *G. fanwei*, the neural spines of the preserved posterior caudal series are ~8.5 times as tall as their respective centra, a proportion far exceeding that calculated in some other iguanodontians (Fig. 7). These elongate, posterodorsally inclined neural spines would form a high, sail-like structure along the posterior portion of the tail in life (Fig. 10). The presence of a caudal sail is therefore a novel morphology within Iguanodontia and highlights that sail-like structures may have evolved multiple times in Iguanodontia, occurring in different regions of the vertebral series. The discovery of this tail morphology adds to the diversity of iguanodontian body plans, and expands our understanding of evolutionary disparities among hadrosauroids.

The current phylogenetic analysis using maximum parsimony recovers *Gongshuilong fanwei* as one of the earliest branching brachylophosaurin taxa at the base of Saurolophinae, which generally matches the aforesaid inference from osteological evaluations. These different lines of evidence together confirm an early-diverging brachylophosaurin saurolophine identity of *G. fanwei*.

Biogeographical inference of ancestral areas

The geographical origin of Saurolophinae has long been contentious, because of the continuous updates of Asian and North American fossil data and subsequently produced phylogenetic topologies (Gates et al., 2011; Godefroit et al., 2008; Horner et al., 2004; H. Xing, Zhao et al., 2014). Nevertheless, some recent studies using statistical analytical approaches have yielded convergent results that supported a predominant North American origin of Saurolophinae: the dispersal-vicariance (DIVA) and dispersal-extinction-cladogenesis (DEC) analyses both regarded North America as the most probable ancestral area for Saurolophinae (Kobayashi et al., 2019; Prieto-Márquez, 2010a); similarly, the probability calculation of ancestral areas indicated a substantially higher possibility for a North American origin of Saurolophinae (~81%), when compared with Asia (~17%) (H. Xing et al., 2017). This hypothesis, namely that the ancestral area of Saurolophinae was limited to North America, is in fact discordant with the broader biogeographical context of Hadrosauroidea and recent discoveries regarding some Asian saurolophines: most non-hadrosaurid hadrosauroids (e.g. *Equijubus normani*, *Bactrosaurus johnsoni*, *Gilmoreosaurus mongoliensis*, *Tanius sinensis* and *Zhanghenglong yangchengensis*) were recovered from Asia (Borinder et al., 2021; Godefroit et al., 2008; Prieto-Márquez, 2011; Prieto-Márquez & Norell, 2010; H. Xing, Wang et al., 2014; You et al., 2003); Lambeosaurinae, the sister taxon to Saurolophinae, is widely recognized to have originated from Asia owing to the presence of multiple Asian early-branching representatives (e.g. *Aralosaurus tuberiferus* and *Jaxartosaurus aralensis*) and convincing results of various biogeographical analyses (Godefroit, Alifanov et al., 2004; Kobayashi et al., 2019; Prieto-Márquez, 2010a; Prieto-Márquez et al., 2012, 2013); *Wulagasaurus* and *Kerberosaurus*, both from the Upper Cretaceous of the Heilongjiang River area, have been confirmed to be among the early-diverging taxa within Brachylophosaurini and Edmontosaurini, respectively (Alarcón-Muñoz et al., 2023; Bolotsky & Godefroit, 2004; Godefroit et al., 2008; H. Xing et al., 2017). This incongruity, as well as the uncertain systematic position of *Hadrosaurus foulkii*, has led to a long-term confusion on the biogeographical history of Hadrosauridae and Saurolophinae (H. Xing et al., 2017).

Our BBM analysis for biogeographical reconstruction provides new perspectives on the ancestral areas of Saurolophinae and its major subclades. The node of Saurolophinae shows an independent probability of ∼79% for North American origin, whereas it also reflects a relatively lower independent probability for Asian origin, namely ∼42%. A similar pattern is available for the node of Brachylophosaurini, which has independent probabilities of ∼74% and ∼44% for the North American and Asian origins, respectively. These analytical results indicate a certain ambiguity regarding the ancestral areas and therefore suggest that the traditional biogeographical hypothesis on the North American origins of Saurolophinae and Brachylophosaurini should be reviewed and reconsidered. The possibility of an Asian origin for the two clades has dramatically increased following the discovery of *Gongshuilong fanwei* from the Upper Cretaceous of South China. This alternative now merits further attention and can no longer be regarded as negligible. Despite this, the probability of the North American origin for Saurolophinae and Brachylophosaurini remains essentially higher. This asymmetrical condition may be largely attributed to preservational and sampling biases of fossil material: all saurolophines from Asia are tentatively restricted to the time interval between the late Campanian and the Maastrichtian, and the available material of the Asian brachylophosaurins (i.e. *Wulagasaurus dongi* and *Gongshuilong fanwei*) are substantially disarticulated and poorly preserved (Bell, 2011; Bolotsky & Godefroit, 2004; Godefroit et al., 2008; H. Xing et al., 2012, H. Xing, Zhao et al., 2014; Zhang et al., 2019). Consequently, the current phylogenetic framework of Saurolophinae is obviously constrained by the relatively incomplete fossil record from Asia. To further clarify the evolutionary and biogeographical history of Saurolophinae and its subclade Brachylophosaurini, the collection of additional well-preserved *Wulagasaurus* and *Gongshuilong* material is required, along with the discovery of pre-Maastrichtian brachylophosaurins in Asia.

Conclusions

Gongshuilong fanwei gen. et sp. nov. is the first formally named hadrosaurid dinosaur from South China, and is the second brachylophosaurin taxon found in Asia. The material of the new taxon recovered from the Upper Cretaceous (Maastrichtian) Lianhe Formation of Ganzhou City in Jiangxi Province clearly displays a unique combination of characteristics, including some salient traits typical of Saurolophinae, some meaningful features common among brachylophosaurins but rarely mentioned in other saurolophines, several interesting characters mainly present in non-saurolophine hadrosauroids, and a probable autapomorphy (i.e. greatly elongate, moderately recurved, posterodorsally directed neural spines of the posterior caudal vertebrae that are ∼8.5 times as tall as their corresponding centra). The strict consensus tree of Hadrosauroidea resulting from the maximum parsimony analysis possesses an unresolved polytomy at the base of Brachylophosaurini within Saurolophinae, which is constituted by *Wulagasaurus*, *Gongshuilong*, *Acristavus* and the clade of *Maiasaura* + (*Probrachylophosaurus* + *Brachylophosaurus*). The result of the BBM analysis incorporating *G. fanwei* increases the possibility of an Asian origin for Brachylophosaurini and Saurolophinae, although additional material is required to further clarify this hypothesis. Overall, this discovery offers new insights into the diversity and late evolution of Saurolophinae in Asia.

Acknowledgements

The authors are very grateful to Lishi Xiang, Beijing Wubo Technology Co. Ltd. and Chongzhou Tianyan Museum for fossil preparation, to Qiming Hu for taking and editing photographs of the specimen, to Frankie Bedek for revising the early draft for English grammar, and to Qiongying Wang for restoration art of the taxon. We also sincerely thank the following people for access to specimens under their care: David Evans, Kieran Shepherd, Carl Mehling, Maureen Walsh, Michael Brett-Surman, Ivan Bolotsky, Idersaikhan Damdinsuren, Don Brinkman, Ping Li, Eric Metz, and Tomohiro Nishimura. Thanks also go to two anonymous reviewers and the editors Susannah Maidment and Jordan Mallon for their valuable comments that greatly improved the manuscript. Funding was provided by the National Natural Science Foundation of China (No. 42288201; No. 42372036; No. 42377447), the BJAST Young Scholar Program (No. 24CE-YS-01), the special financial support of the BJAST and the Beijing Government, and the Yunnan Revitalization Talent Support Program (202305AB350006).

Disclosure statement

No potential conflict of interest was reported by the author(s).

Supplemental material

Supplemental material for this article can be accessed here: https://doi.org/10.1080/14772019.2026.2635569.

Data availability statement

The phylogenetic data (matrix and character list) supporting the findings of this study are available from MorphoBank at https://doi.org/10.7934/P6246 (Yao et al., 2026)

References

Alarcón-Muñoz, J., **Vargas, A. O.**, **Püschel, H. P.**, **Soto-Acuña, S.**, **Manríquez, L.**, **Leppe, M.**, **Kaluza, J.**, **Milla, V.**, **Gutstein, C. S.**, **Palma-Liberona, J.**, **Stinnesbeck, W.**, **Frey, E.**, **Pino, J. P.**, **Bajor, D.**, **Núñez, E.**, **Ortiz, H.**, **Rubilar-Rogers, D.**, & **Cruzado-Caballero, P.** (2023). Relict duck-billed dinosaurs survived into the last age of the dinosaurs in subantarctic Chile. *Science Advances*, *9*, eadg2456. https://doi.org/10.1126/sciadv.adg2456

Bell, P. R. (2011). Cranial osteology and ontogeny of *Saurolophus angustirostris* from the Late Cretaceous of Mongolia with comments on *Saurolophus osborni* from Canada. *Acta Palaeontologica Polonica*, *56*, 703–722. https://doi.org/10.4202/app.2010.0061

Bertozzo, F., **Dalla Vecchia, F. M.**, & **Fabbri, M.** (2017). The Venice specimen of *Ouranosaurus nigeriensis* (Dinosauria, Ornithopoda). *PeerJ*, *5*, e3403. https://doi.org/10.7717/peerj.3403

Bolotsky, Y. L., & **Godefroit, P.** (2004). A new hadrosaurine dinosaur from the Late Cretaceous of Far Eastern Russia. *Journal of Vertebrate Paleontology*, *24*, 351–365. https://doi.org/10.1671/1110

Borinder, N. H., **Poropat, S. F.**, **Campione, N. E.**, **Wigren, T.**, & **Kear, B. P.** (2021). Postcranial osteology of the basally branching hadrosauroid dinosaur *Tanius sinensis* from the Upper Cretaceous Wangshi Group of Shandong, China. *Journal of Vertebrate Paleontology*, *41*, e1914642. https://doi.org/10.1080/02724634.2021.1914642

Brett-Surman, M. K. (1989). A revision of the Hadrosauridae (Reptilia: Ornithischia) and their evolution during the Campanian and Maastrichtian. [Unpublished PhD thesis, George Washington University].

Brown, B. (1913). *A new trachodont dinosaur*, Hypacrosaurus*, from the Edmonton Cretaceous of Alberta*. American Museum of Natural History.

Chen, L., **Steel, R. J.**, **Guo, F.**, **Olariu, C.**, & **Gong, C.** (2016). Alluvial fan facies of the Yongchong Basin: Implications for tectonic and paleoclimatic changes during the Late Cretaceous in SE China. *Journal of Asian Earth Sciences*, *115*, 258–276. https://doi.org/10.1016/j.jseaes.2016.10.010

Currie, P. J., **Nadon, G. C.**, & **Lockley, M. G.** (1991). Dinosaur footprints with skin impressions from the Cretaceous of Alberta and Colorado. *Canadian Journal of Earth Sciences*, *28*, 102–115. https://doi.org/10.1139/e91-009

Cuthbertson, R. S., & **Holmes, R. B.** (2010). The first complete description of the holotype of *Brachylophosaurus canadensis* Sternberg, 1953 (Dinosauria: Hadrosauridae) with comments on intraspecific variation. *Zoological Journal of the Linnean Society*, *159*(2), 373–397. https://doi.org/10.1111/j.1096-3642.2009.00612.x

Cuthbertson, R. S., **Tirabasso, A.**, **Rybczynski, N.**, & **Holmes, R. B.** (2012). Kinetic limitations of intracranial joints in *Brachylophosaurus canadensis* and *Edmontosaurus regalis* (Dinosauria, Hadrosauridae), and their implications for the chewing mechanics of hadrosaurids. *The Anatomical Record*, *295*, 968–979. https://doi.org/10.1002/ar.22458

Dai, H., **Ma, Q.**, **Xiong, C.**, **Lin, Y.**, **Zeng, H.**, **Tan, C.**, **Wang, J.**, **Zhang, Y.**, & **Xing, H.** (2025). A new late-diverging non-hadrosaurid hadrosauroid (Dinosauria: Ornithopoda) from southwest China: Support for interchange of dinosaur faunas across East Asia during the Late Cretaceous. *Cretaceous Research*, *166*, 105995. https://doi.org/10.1016/j.cretres.2024.105995

Dilkes, D. W. (1999). Appendicular myology of the hadrosaurian dinosaur *Maiasaura peeblesorum* from the Late Cretaceous (Campanian) of Montana. *Transactions of the Royal Society of Edinburgh, Earth Sciences*, *90*, 87–125. https://doi.org/10.1017/S0263593300007185

Evans, D. C., & **Reisz, R. R.** (2007). Anatomy and relationships of *Lambeosaurus magnicristatus*, a crested hadrosaurid dinosaur (Ornithischia) from the Dinosaur Park Formation, Alberta. *Journal of Vertebrate Paleontology*, *27*, 373–393. https://doi.org/10.1671/0272-4634(2007)27[373:AAROLM]2.0.CO;2

Freedman Fowler, E. A., & **Horner, J. R.** (2015). A new brachylophosaurin hadrosaur (Dinosauria: Ornithischia) with an intermediate nasal crest from the Campanian Judith River Formation of northcentral Montana Friedman, M. (ed.). *PLoS ONE*, *10*, e0141304. https://doi.org/10.1371/journal.pone.0141304

Gates, T. A., **Horner, J. R.**, **Hanna, R. R.**, & **Nelson, C. R.** (2011). New unadorned hadrosaurine hadrosaurid (Dinosauria, Ornithopoda) from the Campanian of North America. *Journal of Vertebrate Paleontology*, *31*, 798–811. https://doi.org/10.1080/02724634.2011.577854

Gates, T. A., & **Sampson, S. D.** (2007). A new species of *Gryposaurus* (Dinosauria: Hadrosauridae) from the Late Campanian Kaiparowits Formation, southern Utah, USA.

Zoological Journal of the Linnean Society, *151*, 351–376. https://doi.org/10.1111/j.1096-3642.2007.00349.x

Gates, T. A., **Sampson, S. D.**, **De Jesús, C. R. D.**, **Zanno, L. E.**, **Eberth, D.**, **Hernandez-Rivera, R.**, **Martínez, M. C. A.**, & **Kirkland, J. I.** (2007). *Velafrons coahuilensis*, a new lambeosaurine hadrosaurid (Dinosauria: Ornithopoda) from the Late Campanian Cerro del Pueblo Formation, Coahuila, Mexico. *Journal of Vertebrate Paleontology*, *27*, 917–930. https://doi.org/10.1671/0272-4634(2007)27[917:VCANLH]2.0.CO;2

Godefroit, P., **Alifanov, V.**, & **Bolotsky, Y.** (2004). A re-appraisal of *Aralosaurus tuberiferus* (Dinosauria, Hadrosauridae) from the Late Cretaceous of Kazakhstan. *Bulletin de l'Institut royal des Sciences naturelles de Belgique, Sciences de la Terre*, *74*, 139–154. https://doi.org/10.1080/02724631003763508

Godefroit, P., **Bolotsky, Y. L.**, & **Bolotsky, I. Y.** (2012). Osteology and relationships of *Olorotitan arharensis*, a hollow-crested hadrosaurid dinosaur from the Latest Cretaceous of Far Eastern Russia. *Acta Palaeontologica Polonica*, *57*, 527–560. https://doi.org/10.4202/app.2011.0051

Godefroit, P., **Bolotsky, Y. L.**, & **Van Itterbeeck, J.** (2004). The lambeosaurine dinosaur *Amurosaurus riabinini*, from the Maastrichtian of Far Eastern Russia. *Acta Palaeontologica Polonica*, *49*(4), 585–618. https://doi.org/10.4202/app.2011.0051

Godefroit, P., **Hai, S.**, **Yu, T.**, & **Lauters, P.** (2008). New hadrosaurid dinosaurs from the Uppermost Cretaceous of northeastern China. *Acta Palaeontologica Polonica*, *53*, 47–74. https://doi.org/10.4202/app.2008.0103

Godefroit, P., **Lauters, P.**, & **Itterbeeck, J. V.** (2011). Recent advances on study of hadrosaurid dinosaurs in Heilongjiang (Amur) River area between China and Russia. *Global Geology*, *14*(3), 160–191. https://doi.org/10.3969/j.issn.1673-9736.2011.03.03

Godefroit, P., **Zan, S.**, & **Jin, L.** (2000). *Charonosaurus jiayinensis* n.g., n.sp., a lambeosaurine dinosaur from the Late Maastrichtian of northeastern China. *Comptes Rendus de l'Académie des Sciences – Series IIA – Earth and Planetary Science*, *330*, 875–882. https://doi.org/10.1016/S1251-8050(00)00214-7

Goloboff, P. A., & **Morales, M. E.** (2023). TNT version 1.6, with a graphical interface for MacOS and Linux, including new routines in parallel. *Cladistics*, *39*, 144–153. https://doi.org/10.1111/cla.12524

Han, F., **Yang, L.**, **Lou, F.**, **Sullivan, C.**, **Xu, X.**, **Qiu, W.**, **Liu, H.**, **Yu, J.**, **Wu, R.**, **Ke, Y.**, **Xu, M.**, **Hu, J.**, & **Lu, P.** (2024). A new titanosaurian sauropod, *Gandititan cavocaudatus* gen. et sp. nov., from the Late Cretaceous of southern China. *Journal of Systematic Palaeontology*, *22*, 2293038. https://doi.org/10.1080/14772019.2023.2293038

Horner, J. R. (1983). Cranial osteology and morphology of the type specimen of *Maiasaura peeblesorum* (Ornithischia: Hadrosauridae), with a discussion of its phylogenetic position. *Journal of Vertebrate Paleontology*, *3*, 29–38. https://doi.org/10.1080/02724634.1983.10011954

Horner, J. R., **Weishampel, D. B.**, & **Forster, C. A.** (2004). 20. Hadrosauridae. In D. B. Weishampel, P. Dodson, & H. Osmólska (Eds.), *The Dinosauria*, Second Edition (pp. 438–463). University of California Press.

Hu, C. (1973). A new hadrosaur from the Cretaceous of Chucheng, Shantung. *Acta Geologica Sinica*, *2*, 179–206.

Hu, J., & **Han, F.** (2021). A new multituberculate, *Yubaatar qianzhouensis* sp. nov.: The first Late Cretaceous mammal from Ganzhou basin, Jiangxi Province. *Acta Palaeontol Sinica*, *60*, 2020057. https://doi.org/10.19800/j.cnki.aps.2020057

Jin, X., **Mao, F.**, **Du, T.**, **Yang, Y.**, & **Meng, J.** (2023). A new multituberculate from the Latest Cretaceous of central China and its implications for multituberculate tooth homologies and occlusion. *Journal of Mammalian Evolution*, *30*, 1–20. https://doi.org/10.1007/s10914-022-09636-2

Ke, Y., **Niu, K.**, **Rummy, P.**, **Tong, H.**, **Hu, J.**, & **Han, F.** (2024). *Xianyuechelys yingliangi*: A new nanhsiungchelyid turtle from the Late Cretaceous of Ganzhou basin, China. *Journal of Systematic Palaeontology*, *22*, 2346838. https://doi.org/10.1080/14772019.2024.2346838

Kobayashi, Y., **Nishimura, T.**, **Takasaki, R.**, **Chiba, K.**, **Fiorillo, A. R.**, **Tanaka, K.**, **Chinzorig, T.**, **Sato, T.**, & **Sakurai, K.** (2019). A new Hadrosaurine (Dinosauria: Hadrosauridae) from the marine deposits of the Late Cretaceous Hakobuchi Formation, Yezo Group, Japan. *Scientific Reports*, *9*, 12389. https://doi.org/10.1038/s41598-019-48607-1

de Lapparent, A., & **Lavocat, R.** (1955). Dinosauriens. *Traité de paléontologie*, *5*, 785–962.

Li, C., **Wu, X.**, & **Rufolo, S. J.** (2019). A new crocodyloid (Eusuchia: Crocodylia) from the Upper Cretaceous of China. *Cretaceous Research*, *94*, 25–39. https://doi.org/10.1016/j.cretres.2018.09.015

Li, T., **Ding, X.**, **Xiao, Q.**, **Lu, M.**, **Yu, J.**, & **Zhang, Z.** (2017). *Regional geology of China, Jiangxi Province*. Geological Publishing House.

Ling, L. (1996). Establishment of the Cretaceous Maodian, Hekou, and the Tangbian formations in Jiangxi Province. *Geological Science and Technology of Jiangxi*, *23*, 55–59.

Longrich, N. R., **Suberbiola, X. P.**, **Pyron, R. A.**, & **Jalil, N.-E.** (2021). The first duckbill dinosaur (Hadrosauridae: Lambeosaurinae) from Africa and the role of oceanic dispersal in dinosaur biogeography. *Cretaceous Research*, *120*, 104678. https://doi.org/10.1016/10.1016/j.cretres.2020.104678

Lü, J., **Chen, R.**, **Brusatte, S. L.**, **Zhu, Y.**, & **Shen, C.** (2016). A Late Cretaceous diversification of Asian oviraptorid dinosaurs: Evidence from a new species preserved in an unusual posture. *Scientific Reports*, *6*, 35780. https://doi.org/10.1038/srep35780

Lü, J., **Yi, L.**, **Zhong, H.**, & **Wei, X.** (2013). A new oviraptorosaur (Dinosauria: Oviraptorosauria) from the Late Cretaceous of southern China and its paleoecological implications. *PLoS ONE*, *8*, e80557. https://doi.org/10.1371/journal.pone.0080557

Lull, R. S., & **Wright, N. E.** (1942). *Hadrosaurian dinosaurs of North America*. Geological Society of America Special Papers. Geological Society of America. https://doi.org/10.1130/spe40-p1

Lund, E. K., & **Gates, T. A.** (2006). A historical and biogeographical examination of hadrosaurian dinosaurs. *New Mexico Museum of Natural History and Science Bulletin*, *35*, 263–276.

Maryanska, T., & **Osmólska, H.** (1981). First lambeosaurine dinosaur from the Nemegt Formation, Upper Cretaceous, Mongolia. *Acta Palaeontologica Polonica*, *26*(3–4), 243–255.

Maryanska, T., & **Osmólska, H.** (1984). Postcranial anatomy of *Saurolophus angustirostris* with comments on other hadrosaurs. *Palaeontologia Polonica*, *46*, 119–141.

McDonald, A. T., **Bird, J.**, **Kirkland, J. I.**, & **Dodson, P.** (2012). Osteology of the basal hadrosauroid *Eolambia caroljonesa* (Dinosauria: Ornithopoda) from the Cedar Mountain Formation of Utah. *PLoS ONE*, *7*, e45712. https://doi.org/10.1371/journal.pone.0045712

Nabavizadeh, A. (2016). Evolutionary trends in the jaw adductor mechanics of ornithischian dinosaurs. *The Anatomical Record*, *299*, 271–294. https://doi.org/10.1002/ar.23306

Norman, D. B. (2004). Basal Iguanodontia. In D. B. Weishampel, P. Dodson, & H. Osmólska (Eds.), *The Dinosauria*, Second Edition (pp. 413–437). University of California Press. https://doi.org/10.1525/9780520941434-025

Ostrom, J. H. (1961). Cranial morphology of the hadrosaurian dinosaurs of North America. *Bulletin of the American Museum of Natural History*, *122*, 37.

Prieto-Márquez, A. (2005). New information on the cranium of *Brachylophosaurus canadensis* (Dinosauria, Hadrosauridae), with a revision of its phylogenetic position. *Journal of Vertebrate Paleontology*, *25*, 144–156. https://doi.org/10.1671/0272-4634(2005)025[0144:niotco]2.0.co;2

Prieto-Márquez, A. (2008). Phylogeny and historical biogeography of hadrosaurid dinosaurs. [PhD dissertation, Florida State University, Tallahassee].

Prieto-Márquez, A. (2010a). Global historical biogeography of hadrosaurid dinosaurs: Biogeography of Hadrosauridae. *Zoological Journal of the Linnean Society*, *159*, 503–525. https://doi.org/10.1111/j.1096-3642.2010.00642.x

Prieto-Márquez, A. (2010b). Global phylogeny of Hadrosauridae (Dinosauria: Ornithopoda) using parsimony and Bayesian methods: Phylogeny of hadrosaurid dinosaurs. *Zoological Journal of the Linnean Society*, *159*, 435–502. https://doi.org/10.1111/j.1096-3642.2009.00617.x

Prieto-Márquez, A. (2011). Cranial and appendicular ontogeny of *Bactrosaurus johnsoni*, a hadrosauroid dinosaur from the Late Cretaceous of northern China. *Palaeontology*, *54*, 773–792. https://doi.org/10.1111/j.1475-4983.2011.01053.x

Prieto-Márquez, A. (2012). The skull and appendicular skeleton of *Gryposaurus latidens*, a saurolophine hadrosaurid (Dinosauria: Ornithopoda) from the Early Campanian (Cretaceous) of Montana, USA. *Canadian Journal of Earth Sciences*, *49*, 510–532. https://doi.org/10.1139/e11-069

Prieto-Márquez, A. (2014). Skeletal morphology of *Kritosaurus navajovius* (Dinosauria: Hadrosauridae) from the Late Cretaceous of the North American south-west, with an evaluation of the phylogenetic systematics and biogeography of Kritosaurini. *Journal of Systematic Palaeontology*, *12*, 133–175. https://doi.org/10.1080/14772019.2013.770417

Prieto-Márquez, A., **Chiappe, L. M.**, & **Joshi, S. H.** (2012). The lambeosaurine dinosaur *Magnapaulia laticaudus* from the Late Cretaceous of Baja California, northwestern Mexico. *PLoS ONE*, *7*, e38207. https://doi.org/10.1371/journal.pone.0038207

Prieto-Márquez, A., **Dalla Vecchia, F. M.**, **Gaete, R.**, & **Galobart, À.** (2013). Diversity, relationships, and biogeography of the lambeosaurine dinosaurs from the European Archipelago, with description of the new aralosaurin *Canardia garonnensis PLoS ONE*, *8*, e69835. https://doi.org/10.1371/journal.pone.0069835

Prieto-Márquez, A., **Erickson, G. M.**, & **Ebersole, J. A.** (2016). Anatomy and osteohistology of the basal hadrosaurid dinosaur *Eotrachodon* from the uppermost Santonian (Cretaceous) of southern Appalachia. *PeerJ*, *4*, e1872. https://doi.org/10.7717/peerj.1872

Prieto-Márquez, A., & **Guenther, M. F.** (2018). Perinatal specimens of *Maiasaura* from the Upper Cretaceous of Montana (USA): Insights into the early ontogeny of saurolophine hadrosaurid dinosaurs. *PeerJ*, *6*, e4734. https://doi.org/10.7717/peerj.4734

Prieto-Márquez, A., & **Norell, M. A.** (2010). Anatomy and relationships of *Gilmoreosaurus mongoliensis* (Dinosauria: Hadrosauroidea) from the Late Cretaceous of central Asia. *American Museum Novitates*, *3694*, 1–49. https://doi.org/10.7717/10.1206/3694.2

Prieto-Márquez, A., & **Wagner, J. R.** (2009). *Pararhabdodon isonensis* and *Tsintaosaurus spinorhinus*: A new clade of lambeosaurine hadrosaurids from Eurasia. *Cretaceous Research*, *30*(5), 1238–1246. https://doi.org/10.1016/j.cretres.2009.06.005

Prieto-Márquez, A., **Wagner, J. R.**, **Bell, P. R.**, & **Chiappe, L. M.** (2015). The late-surviving 'duck-billed' dinosaur *Augustynolophus* from the Upper Maastrichtian of western North America and crest evolution in Saurolophini. *Geological Magazine*, *152*, 225–241. https://doi.org/10.1017/S0016756814000284

Rozhdestvensky, A. K. (1968). *Hadrosaurs of Kazakhstan*. In L. P. Tatarinov, P. K. Chudinov, & M. A. Shishkin (Eds.), *Upper Paleozoic and Mesozoic amphibians and reptiles* (pp. 97–141). Akademia Nauk S.S.S.R. (In Russian).

Rybczynski, N., **Tirabasso, A.**, **Bloskie, P.**, **Cuthbertson, R.**, & **Holliday, C.** (2008). A three-dimensional animation model of *Edmontosaurus* (Hadrosauridae) for testing chewing hypotheses. *Palaeontologia Electronica*, *11*, 1–14.

Takasaki, R., **Chiba, K.**, **Fiorillo, A. R.**, **Brink, K. S.**, **Evans, D. C.**, **Fanti, F.**, **Saneyoshi, M.**, **Maltese, A.**, & **Ishigaki, S.** (2023). Description of the first definitive *Corythosaurus* (Dinosauria, Hadrosauridae) specimens from the Judith River Formation in Montana, USA and their paleobiogeographical significance. *Anatomical Record*, *306*, 1918–1938. https://doi.org/10.1002/ar.25097

Tsogtbaatar, K., **Weishampel, D. B.**, **Evans, D. C.**, & **Watabe, M.** (2019). A new hadrosauroid (Dinosauria: Ornithopoda) from the Late Cretaceous Baynshire Formation of the Gobi Desert (Mongolia) Mpodozis, J. M. (ed.). *PLoS ONE*, *14*, e0208480. https://doi.org/10.1371/journal.pone.0208480

Wang, M., **Dong, L.**, **Yu, J.**, **Lou, F.**, **Qiu, W.**, & **Han, F.** (2025). A new borioteiioid lizard with large caniniform tooth from the Upper Cretaceous of south China. *Journal of Systematic Palaeontology*, *23*, 2509637. https://doi.org/10.1080/14772019.2025.2509637

Wang, X., & **Xu, X.** (2001). A new iguanodontid (*Jinzhousaurus yangi* gen. et sp. nov.) from the Yixian Formation of western Liaoning, China. *Chinese Science Bulletin*, *46*, 1669–1672. https://doi.org/10.1007/BF02900633

Wei, X., **Pu, H.**, **Xu, L.**, **Liu, D.**, & **Lü, J.** (2013). A new oviraptorid dinosaur (Theropoda: Oviraptorosauria) from the Late Cretaceous of Jiangxi Province, southern China. *Acta Geologica Sinica – English Edition*, *87*, 899–904. https://doi.org/10.1111/1755-6724.12098

Wing, S. L., & **Sues, H. D.** (1992). Mesozoic and Early Cenozoic terrestrial ecosystems. In A. K. Behrensmeyer, J. D. Damuth, W. A. DiMichele, R. Potts, H. D. Sues, & S. L. Wing (Eds.), *Terrestrial ecosystems through time* (pp. 327–418). University of Chicago Press.

Wu, R., **Lou, F.**, **Yu, J.**, **Xue, Y.**, **Zhang, S.**, **Yang, L.**, **Qiu, W.**, **Wang, H.**, & **Han, F.** (2024). The smallest known complete dinosaur fossil eggs from the Upper Cretaceous of South China. *Historical Biology*, *37*, 2109–2118. https://doi.org/10.1080/08912963.2024.2409873

Wu, R., **Niu, K.**, **Zhang, S.**, **Xue, Y.**, & **Han, F.** (2024). A new ootype of putative dromaeosaurid eggs from the Upper Cretaceous of southern China. *Cretaceous Research*, *161*, 105909. https://doi.org/10.1016/j.cretres.2024.105909

Wu, X. C., **Wang, Y. C.**, **You, H. L.**, **Zhang, Y. Q.**, & **Yi, L.** (2023). New brevirostrines (Crocodylia, Brevirostres) from the Upper Cretaceous of China. *Cretaceous Research*, *144*, 105450. https://doi.org/10.1016/j.cretres.2022.105450

Xi, D., **Sun, L.**, **Qin, Z.**, **Li, G.**, **Li, G.**, & **Wan, X.** (2021). Lithostratigraphic division and correlation of the Cretaceous in China. *Journal of Stratigraphy*, *45*, 375–401. https://doi.org/10.1671/0272-4634-28.4.1073

Xiao, G., **Fan, A.**, & **Yao, Q.** (2013). Study on sequence stratigraphy of the Late Cretaceous in Jiangxi Province. *Resource Survey and Environment*, *34*, 141–149.

Xing, H., **Gu, W.**, **Hai, S.**, **Yu, T.**, **Han, D.**, **Zhang, Y.**, & **Zhang, S.** (2021). Osteological and taxonomic reassessments of *Sahaliyania elunchunorum* (Dinosauria, Hadrosauridae) from the Upper Cretaceous Yuliangzi Formation, northeast China. *Journal of Vertebrate Paleontology*, *41*, e2085111. https://doi.org/10.1080/02724634.2021.2085111

Xing, H., **Mallon, J. C.**, & **Currie, M. L.** (2017). Supplementary cranial description of the types of *Edmontosaurus regalis* (Ornithischia: Hadrosauridae), with comments on the phylogenetics and biogeography of Hadrosaurinae Fiorillo, A. (ed.). *PLoS ONE*, *12*, e0175253. https://doi.org/10.1371/journal.pone.0175253

Xing, H., **Prieto-Márquez, A.**, **Gu, W.**, & **Yu, T.** (2012). Reevaluation and phylogenetic analysis of the hadrosaurine dinosaur *Wulagasaurus dongi* from the Maastrichtian of northeast China. *Vertebrata PalAsiatica*, *50*, 160.

Xing, H., **Wang, D.**, **Han, F.**, **Sullivan, C.**, **Ma, Q.**, **He, Y.**, **Hone, D. W. E.**, **Yan, R.**, **Du, F.**, & **Xu, X.** (2014). A new basal hadrosauroid dinosaur (Dinosauria: Ornithopoda) with transitional features from the Late Cretaceous of Henan Province, China. *PLoS ONE*, *9*, e98821. https://doi.org/10.1371/journal.pone.0098821

Xing, H., **Zhao, X.**, **Wang, K.**, **Li, D.**, **Chen, S.**, **Mallon, J. C.**, **Zhang, Y.**, & **Xu, X.** (2014). Comparative osteology and phylogenetic relationship of *Edmontosaurus* and *Shantungosaurus* (Dinosauria: Hadrosauridae) from the Upper Cretaceous of North America and East Asia. *Acta Geologica Sinica – English Edition*, *88*, 1623–1652. https://doi.org/10.1111/1755-6724.12334

Xing, L., **Niu, K.**, & **Evans, S. E.** (2023). A new polyglyphanodontian lizard with a complete lower temporal bar from the Upper Cretaceous of southern China. *Journal of Systematic Palaeontology*, *21*, 2281494. https://doi.org/10.1080/14772019.2023.2281494

Xing, L., **Niu, K.**, **Wang, D.**, & **Márquez, A. P.** (2021). A partial articulated hadrosaurid skeleton from the Maastrichtian (Upper Cretaceous) of the Ganzhou area, Jiangxi Province, China. *Historical Biology*, *33*, 2256–2259. https://doi.org/10.1080/08912963.2020.1782397

Xing, L., **Niu, K.**, **Yang, T.**, **Wang, D.**, **Miyashita, T.**, & **Mallon, J. C.** (2022). Hadrosauroid eggs and embryos from the Upper Cretaceous (Maastrichtian) of Jiangxi Province, China. *BMC Ecology and Evolution*, *22*, 60. https://doi.org/10.1186/s12862-022-02012-x

Xing, L., **Niu, K.**, **Zhang, L.**, **Yang, T.**, **Zhang, J.**, **Persons Iv, W. S.**, **Romilio, A.**, **Zhuang, Y.**, & **Ran, H.** (2020). Dinosaur eggs associated with crustacean trace fossils from the Upper Cretaceous of Jiangxi, China: Evidence for foraging behavior? *Biosis:Biological Systems*, *1*(2), 54–59. https://doi.org/10.37819/biosis.001.002.0058

Yang, C. (1973). On a Mesozoic lizard from Kanhsien, Kiangsi. *Vertebrata PalAsiatica*, *11*(1), 44–45.

Yang, Z. (1958). *The Dinosaurian remains of Laiyang, Shantung*. Science Press, Palaeontologia Sinica.

Yao, H., **Qiu, W.**, **Yu, J.**, **Yang, L.**, **Wang, H.**, **Cao, S.**, **Zhao, K.**, **Xu, M.**, **Shi, G.**, **Lou, F.**, **Zeng, C.**, **Lu, P.**, **Wu, R.**, **Xu, X.**, **Han, F.**, & **Xing, H.** (2026). Project 6246: A new saurolophine hadrosaurid (Dinosauria: Ornithopoda) from the Upper Cretaceous of South China, providing further support for the possible Asian origin of Brachylophosaurini [dataset]. *MorphoBank*. https://doi.org/10.7934/P6246

You, H., **Luo, Z.**, **Shubin, N. H.**, **Witmer, L. M.**, **Tang, Z.**, & **Tang, F.** (2003). The earliest-known duck-billed dinosaur from deposits of Late Early Cretaceous age in northwest China and hadrosaur evolution. *Cretaceous Research*, *24*, 347–355. https://doi.org/10.1080/10.1016/S0195-6671(03)00048-X

Yu, Y., **Blair, C.**, & **He, X.** (2020). RASP 4: Ancestral state reconstruction tool for multiple genes and characters. *Molecular Biology and Evolution*, *37*, 604–606. https://doi.org/10.1093/molbev/msz257

Zhang, J., **Wang, X.**, **Jiang, S.**, & **Li, G.** (2021). Internal morphology of nasal spine of *Tsintaosaurus spinorhinus* (Ornithischia: Lambeosaurinae) from the Upper Cretaceous of Shandong, China. *Historical Biology*, *33*, 1697–1704. https://doi.org/10.1080/08912963.2020.1731804

Zhang, J., **Wang, X.**, **Wang, Q.**, **Jiang, S.**, **Cheng, X.**, **Li, N.**, & **Qiu, R.** (2019). A new saurolophine hadrosaurid (Dinosauria: Ornithopoda) from the Upper Cretaceous of Shandong, China. *Anais da Academia Brasileira de Ciências*, *91*, e20160920. https://doi.org/10.1590/0001-3765201720160920

Zheng, W., **Jin, X.**, **Xie, J.**, & **Du, T.** (2024). The first deep-snouted tyrannosaur from Upper Cretaceous Ganzhou city of southeastern China. *Scientific Reports*, *14*, 16276. https://doi.org/10.1038/s41598-024-66278-5

Zhong, C., **Xu, P.**, **Xiao, X.**, **Wang, D.**, & **Long, T.** (2002). Revision of the Late Cretaceous Maodian Formation of the Ganzhou group in Jiangxi Province. Geology in China, *29*, 271–274.

Associate Editor: Dr Jordan Mallon